AD_____

Award Number: DAMD17-03-1-0325

TITLE: p190-B, A Novel RhoGAP, In Mammary Gland Development and Breast Cancer Progression

PRINCIPAL INVESTIGATOR: Tracy Vargo-Gogola, Ph.D.
Jeffrey M. Rosen, Ph.D.

CONTRACTING ORGANIZATION: Baylor College of Medicine
Houston TX 77030

REPORT DATE: September 2006

TYPE OF REPORT: Annual Summary

PREPARED FOR: U.S. Army Medical Research and Materiel Command
Fort Detrick, Maryland 21702-5012

REPORT DOCUMENTATION PAGE

Form Approved
OMB No. 0704-0188

1. REPORT DATE *(DD-MM-YYYY)*	**2. REPORT TYPE**	**3. DATES COVERED** *(From - To)*
01-09-2006	Annual Summary	01 Sep 03 – 31 Aug 06

4. TITLE AND SUBTITLE
p190-B, A Novel RhoGAP, In Mammary Gland Development and Breast Cancer Progression

5a. CONTRACT NUMBER

5b. GRANT NUMBER
DAMD17-03-1-0325

5c. PROGRAM ELEMENT NUMBER

6. AUTHOR(S)
Tracy Vargo-Gogola, Ph.D.; Jeffrey M. Rosen, Ph.D.

E-Mail: tracyv@bcm.edu

5d. PROJECT NUMBER

5e. TASK NUMBER

5f. WORK UNIT NUMBER

7. PERFORMING ORGANIZATION NAME(S) AND ADDRESS(ES)

Baylor College of Medicine
Houston TX 77030

8. PERFORMING ORGANIZATION REPORT NUMBER

9. SPONSORING / MONITORING AGENCY NAME(S) AND ADDRESS(ES)
U.S. Army Medical Research and Materiel Command
Fort Detrick, Maryland 21702-5012

10. SPONSOR/MONITOR'S ACRONYM(S)

11. SPONSOR/MONITOR'S REPORT NUMBER(S)

12. DISTRIBUTION / AVAILABILITY STATEMENT
Approved for Public Release; Distribution Unlimited

13. SUPPLEMENTARY NOTES

14. ABSTRACT:
We have examined the effects of loss and gain of p190-B RhoGAP function on embryonic and postnatal mammary gland development, respectively. Using inducible p190-B overexpressing mice, we have shown that p190-B plays an essential role in the developing mammary gland by regulating both mammary epithelial cell behavior and the microenvironment. Interestingly, overexpression of p190-B during pregnancy results in hyperplastic lesions suggesting that p190-B may affect breast tumorigenesis. P190-B is also required for embryonic mammary gland development because homozygous deletion of p190-B results in smaller buds with diminished mesenchyme. Interactions between the p190-B and IGF-IR signaling pathways affect both embryonic and postnatal mammary gland development. Finally, using inducible p190-B overexpressing MCF-7 human breast cancer cells we have demonstrated a novel role for p190-B as a regulator of mitosis and cytokinesis. Overexpression of p190-B leads to failed cytokinesis, multinucleation, and potentially genomic instability. We propose that this may be one mechanism by which p190-B contributes to breast tumorigenesis.

15. SUBJECT TERMS
p190-B RhoGAP, terminal end buds, ductal morphogenesis, mammary gland development, tumor biology, cell signaling

16. SECURITY CLASSIFICATION OF:			**17. LIMITATION OF ABSTRACT**	**18. NUMBER OF PAGES**	**19a. NAME OF RESPONSIBLE PERSON**
a. REPORT	**b. ABSTRACT**	**c. THIS PAGE**			USAMRMC
U	U	U	UU	59	**19b. TELEPHONE NUMBER** *(include area code)*

Table of Contents

Introduction

During the 3 years of this grant, we generated tet-regulatable p190-B overexpressing transgenic mice. Using these mice, the effects of p190-B overexpression during all stages of mammary gland development was examined. We have also investigated the effects of p190-B loss of function during embryonic mammary gland development. The overexpression studies are now published in *Molecular Endocrinology*. A manuscript describing the embryonic mammary gland development studies has been reviewed by *Developmental Biology* and is now in revision. Together, these two reports complete *Task 1*. Our investigation of the effects of loss and gain of p190-B function on ErbB2-induced mammary tumorigenesis, as proposed in *Task 2*, is in progress as described below. Finally, we have developed inducible p190-B overexpressing MCF-7 human breast cancer cell lines to address the experiments proposed in *Task 3*. Using this model we have identified a novel role for p190-B in regulating mitosis and cytokinesis, and overexpression of p190-B leads to multinucleation. We propose that this may be one mechanism by which p190-B may influence tumorigenesis potentially by affecting genomic stability.

Body

Task 1. To elucidate the role of p190-B in mammary gland development in p190-B deficient and tetracycline (tet)-regulatable p190-B overexpressing mice (Months 1-24).

The role of p190-B in mammary gland development using the tet-regulatable p190-B overexpressing mice has now been published in *Molecular Endocrinology*, and a reprint of the manuscript has been included as Appendix 1. The major findings of these studies are summarized as follows. P190-B Rho GTPase activating protein (GAP) is essential for mammary gland development since p190-B deficiency prevents ductal morphogenesis. To investigate the role of p190-B during distinct stages of mammary gland development, tetracycline (tet)-regulatable p190-B overexpressing mice were generated (Appendix 1, Figure 1). Short-term induction of p190-B in the developing mammary gland results in abnormal terminal end buds (TEBs) that exhibit aberrant budding off the neck, histological anomalies, and a markedly thickened stroma (Appendix 1, Figures 1 and 2). Overexpression of p190-B throughout postnatal development results in increased branching, delayed ductal elongation, and disorganization of the ductal tree (Appendix 1, Figure 6). Interestingly, overexpression of p190-B during pregnancy results in hyperplastic lesions (Appendix 1, Figure 7). Several cellular and molecular alterations detected within the aberrant TEBs may contribute to these phenotypes. Signaling through the insulin-like growth factor (IGF) pathway is altered (Appendix 1, Figure 5), and the myoepithelial cell layer is discontinuous at sites of aberrant budding (Appendix 1, Figure 3). An increase in collagen and extensive infiltration of macrophages, which have recently been implicated in branching morphogenesis, is observed in the stroma surrounding the p190-B overexpressing TEBs (Appendix 1, Figure 4). We propose that the stromal response, disruption of the myoepithelial layer, and alterations in IGF signaling in the p190-B overexpressing mice impact the TEB architecture leading to disorganization and increased branching of the ductal tree. Moreover, we suggest that alterations in tissue architecture and the adjacent stroma as a consequence of p190-B overexpression during pregnancy leads to loss of growth control and the formation of hyperplasia. These data demonstrate that precise control of p190-B RhoGAP activity is critical for normal branching morphogenesis during mammary gland development.

We have also investigated the effects of loss of p190-B function on development of the embryonic mammary gland. These studies were prompted by previous results from our laboratory demonstrating that mammary buds with a homozygous deletion of the p190-B gene do not grow out when transplanted into adult recipient mice. We, therefore, examined the effects of loss of p190-B function on embryonic mammary bud development. These studies, which are summarized below are described in detail in Appendix 2, which is the manuscript that we submitted to *Developmental Biology* and is now in revision.

Embryos with a homozygous p190-B gene deletion exhibit major defects in embryonic mammary bud development. Overall, p190-B deficient buds were smaller in size, contained fewer cells that stained for p63, and displayed characteristics of impaired mesenchymal proliferation and differentiation (Appendix 2, Figures 2 and 3). Consistent with the reported effects of p190-B deletion on IGF-1R signaling, IGF-1R null embryos also displayed a similar small mammary bud phenotype with loss of p63 staining cells (Appendix 2, Figure 4). However, unlike the p190-B null embryos, mesenchymal defects were not detected in the IGF-1R-homozygous embryos. Because p190-B and IGF-IR signaling intersect at the level of the IRS proteins, we examined IRS1/2 double knockout embryonic mammary buds. IRS1/2 double knockout embryos displayed major developmental defects similar to the p190B null embryos including smaller bud size and fewer p63 positive cells (Appendix 2, Figures 5-7). Importantly, like the p190-B deficient buds, the proliferation and differentiation of the IRS1/2 deficient mesenchyme was impaired (Appendix 2, Figure 8). These results indicate that interactions of the p190-B and IGF-1R signaling pathways are critical for embryonic mammary bud development. We suggest that these pathways function in recruiting or maintaining a subset of epithelial progenitors and direct essential epithelial-mesenchymal interactions required to promote mammary bud development.

Task 2. To investigate the role of p190-B in breast cancer progression using both p190-B loss and gain of function mouse models (Months 12-36).

The p190-B deficient mice have been bred to the MMTV-ErbB2 mice to generate 15 MMTV-ErbB2 females with loss of one allele of p190-B. These studies can only be performed with loss of one allele of p190-B because homozygous deletion results in embryonic lethality. There are now approximately 15 mice each in the experimental and control cohorts. We are aiming to have at least 25 mice in each cohort to provide sufficient numbers to obtain statistically significant results. When the mice reach 4-5 months of age we will begin palpating them one time per week to determine tumor latency. Once tumors have formed we will measure tumor growth using calipers twice per week. These are long-term studies, which we expect to complete within the next 12-18 months. We are still in the process of examining the effects of p190-B overexpression on MMTV-ErbB2 induced tumorigenesis. Obtaining trigenic MMTV-rtTA/TetO-p190-B/MMTV-ErbB2 female mice has been challenging, especially because space in our transgenic mouse facility has become severely limited due to construction. In addition, these mice have not bred well under these disruptive conditions, which includes vibrations and noise from the construction that has been underway for the last 6 months. As more trigenic mice are obtained they will be added to the study, which we expect will continue for the next 18-24 months. While we are generating these mice, we will take an alternative approach using MCF-7 tet-regulatable p190-B overexpressing clones in xenograft studies in nude mice. This approach does not require mice to be bred so it can be done in the limited space we have available in our facility. In addition, this allows us to study the effects of p190-B overexpression in a human breast cancer cell line, which has particular relevance to estrogen receptor positive breast cancer.

Task 3. To delineate the molecular mechanism by which p190-B facilitates tumor cell migration and invasion using tet-regulatable p190-B overexpressing MCF7 breast cancer cells (Months 12-36).

For these studies we generated tet-regulatable p190-B overexpressing MCF-7 clones using an HA-tagged p190-B-IRES-luciferase construct. Two clones were chosen, one low expressing clone (clone 48) and one high expressing clone (clone 57) as determined by luciferase assays (data not shown). To investigate the effects of p190-B overexpression on migration, we performed a standard monolayer wound closing assay in which cells were plated at confluency, a scratch was made in the monolayer, and the ability of the cells to migrate into this area to close the wound was measured. When we performed these experiments we noted that the p190-B overexpressing clones, in contrast to the control clone, which migrated into the wounded area, were dying after induction of p190-B (data not shown). As a result, it was not possible to use this assay to measure migration, which is dependent on the cells being confluent. Interestingly, when we examined the morphology of the p190-B overexpressing clones we noticed that there appeared to be cells containing multiple nuclei in the p190-B overexpressing clones as compared to the control clones (data not shown and Figure 2). This observation, together with reports in the literature implicating the Rho signaling network and other RhoGAPs including the related p190-A RhoGAP in regulation of mitosis and cytokinesis (1, 2), prompted us to further examine what role p190-B might be playing in these processes.

To determine the expression patterns of both the endogenous p190-B and the HA-tagged p190-B transgene during mitosis and cytokinesis, immunostaining was performed to detect p190-B and α-tubulin, a component of the mitotic spindle. Analysis of these cells using confocal microscopy showed that both endogenous p190-B as well as the HA-tagged p190-B transgene localize to the mitotic spindle throughout

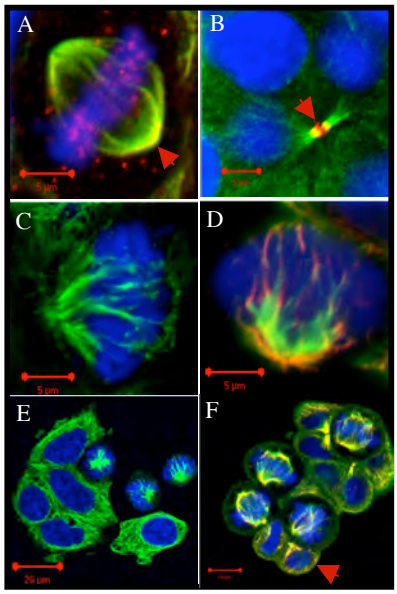

Figure 1: Confocal microscopy images showing expression patterns of endogenous p190-B and the HA-tagged p190-B transgene. A. Endogenous p190-B (red) localizes to the mitotic spindle during metaphase as shown by co-localized staining (yellow, arrow) with αtubulin (green). P190-B also shows punctate staining (red) along the metaphase plate (blue). B. Endogenous p190-B (red) localizes to the midbody (arrow) during cytokinesis. Microtubules are stained green and nuclei are blue. C-F. HA-tagged p190-B transgene expression (red and yellow staining in D,F) localizes to the mitotic spindle (green). Panels C and E are negative controls for the HA-tag staining, which show a metaphase cell from the control clone or a cluster of cells stained with αtubulin and anti-HA antibodies. F. HA-tagged p190-B transgene localizes at the spindle, midbody (white arrow) and membrane (red and yellow, red arrow).

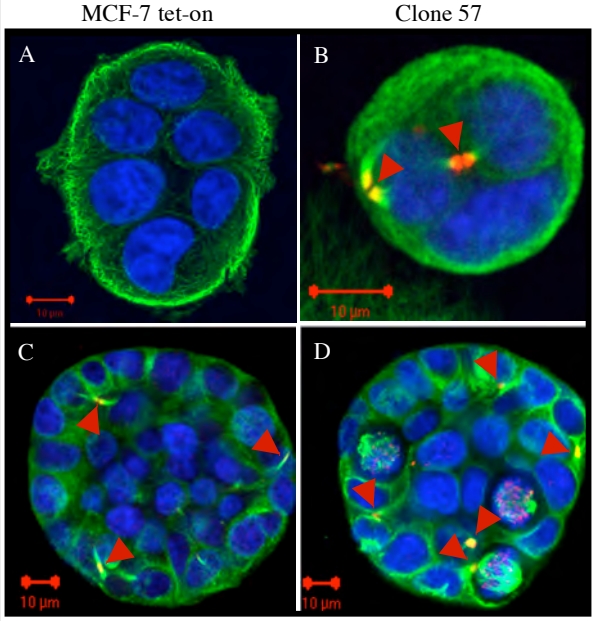

Figure 2: P190-B overexpression results in multinucleation. Confocal microscopy images showing multinucleation of the p190-B overexpressing clone 57 grown in 2D or 3D cultures (panels B and D, respectively) as compared to the control clone (panels A and C). Cells were stained for αtubulin (green), p190-B (red), and with topro-3 to stain nuclei blue. Arrows point to midbodies. Note the increase in the number of midbodies as well as the presence of multiple midbody connections between cells indicating failed cytokinesis and multinucleation in the p190-B overexpressing clone as compared to the control clone.

mitosis and to the midbody during cytokinesis (Figure 1). Interestingly, in contrast to p190-B, p190-A does not localize to the mitotic spindle or to the midbody suggesting that these related family members play distinct roles in mitosis and cytokinesis (2). P190-B overexpression for 48 hours in cells grown on plastic or for 5 days in cells grown in reconstituted basement membrane results in an increase in the number of metaphase cells (4.0% and 4.2% vs. 2.25% for the p190-B overexpressing clones compared to the control clone, respectively, n=~1000 nuclei counted per clone), cells retaining midbodies (13.3% and 16.6% vs. 8.9%, for the p190-B overexpressing clones compared to the control clone, respectively, n=~1000 nuclei counted per clone), and multinucleated cells as shown by representative confocal images of cells containing multiple midbodies (Figure 2B,C arrows). These results are consistent with several published reports demonstrating that inhibition of Rho activity leads to a delay in metaphase and failed cytokinesis (3). Taken together, these data suggest that p190-B may be involved in multiple stages of mitosis, and alteration of p190-B expression is sufficient to disrupt mitosis and cytokinesis thereby giving rise to multinucleated cells. We suggest that this may be one mechanism by which p190-B may contribute to breast tumorigenesis by promoting multinucleation potentially leading to genomic instability. Future studies are aimed at determining the molecular mechanisms by which p190-B regulates mitosis and cytokinesis, and whether overexpression of p190-B enhances the tumorigenicity of MCF-7 cells in xenograft experiments.

References

1. Narumiya S, Yasuda S 2006 Rho GTPases in animal cell mitosis. Curr Opin Cell Biol 18:199-205.
2. Su L, Agati JM, Parsons SJ 2003 p190RhoGAP is cell cycle regulated and affects cytokinesis. J Cell Biol 163:571-82.
3. Wadsworth P 2005 Cytokinesis: Rho marks the spot. Curr Biol 15:R871-4.

Key Research Accomplishments

- A manuscript examining the effects of gain of p190-B function on all stages of postnatal mammary gland development has been published.

- Tet-inducible p190-B overexpressing MCF-7 human breast cancer cell lines have been generated and lead to the discovery of a novel role for p190-B in mitosis and cytokinesis.

Reportable Outcomes

1. A manuscript entitled "P190-B Rho GTPase Activating Protein Overexpression Disrupts Ductal Morphogenesis and Induces Hyperplastic Lesions in the Developing Mammary Gland" by Tracy Vargo-Gogola, Brandy M. Heckman, Edward J. Gunther, Lewis Chodosh, and Jeffrey M. Rosen was published in *Molecular Endocrinology* 20(6):1391-1405.
2. I have been awarded an NCI K99/R00 Howard Temin Pathway to Independence Career Development Award based on the studies funded by this proposal.
3. Based on the work supported by this proposal I have obtained an academic faculty position as an Assistant Professor in the Indiana University School of Medicine at Notre Dame that I will start in January of 2008.

Conclusions

The funding provided by this proposal has been key to my successful completion of several research goals. In addition, I believe that this research and the training that I have received at Baylor College of Medicine has provided me with a strong foundation to direct an independent research program in the areas of mammary gland biology and breast cancer. I look forward to continued interactions and support from the DOD Breast Cancer Research Program in the future.

Appendices

1. "P190-B Rho GTPase Activating Protein Overexpression Disrupts Ductal Morphogenesis and Induces Hyperplastic Lesions in the Developing Mammary Gland" by Tracy Vargo-Gogola, Brandy M. Heckman, Edward J. Gunther, Lewis Chodosh, and Jeffrey M. Rosen, *Molecular Endocrinology* 20(6):1391-1405.
2. "Crosstalk Between the P190-B RhoGAP and IGF Signaling Pathways is Required for Embryonic Mammary Bud Development" by Brandy M. Heckman, Geetika Chakravarty, Tracy Vargo-Gogola, Maria Gonzales-Rimbau, Darryl L. Hadsell, Adrian V. Lee, Jeffrey Settleman, and Jeffrey M. Rosen. *In Revision*.

Contact information:

Tracy Vargo-Gogola, Ph.D.
Department of Molecular and Cellular Biology
Baylor College of Medicine, M637
Houston, TX 77030
Phone 713-798-6211
Fax 713-798-8012

0888-8809/06/$15.00/0
Printed in U.S.A.

Molecular Endocrinology 20(6):1391–1405

doi: 10.1210/me.2005-0426

P190-B Rho GTPase-Activating Protein Overexpression Disrupts Ductal Morphogenesis and Induces Hyperplastic Lesions in the Developing Mammary Gland

Tracy Vargo-Gogola, Brandy M. Heckman, Edward J. Gunther, Lewis A. Chodosh, and Jeffrey M. Rosen

Department of Molecular and Cellular Biology (T.V.-G., B.M.H., J.M.R.), Baylor College of Medicine, Houston, Texas 77030; Jake Gittlen Cancer Foundation (E.J.G.), Penn State College of Medicine, Hershey, Pennsylvania 17033; and Department of Cancer Biology (L.A.C.), Abramson Family Cancer Research Institute, University of Pennsylvania, Philadelphia, Pennsylvania 19104

p190-B Rho GTPase activating protein is essential for mammary gland development because p190-B deficiency prevents ductal morphogenesis. To investigate the role of p190-B during distinct stages of mammary gland development, tetracycline-regulatable p190-B-overexpressing mice were generated. Short-term induction of p190-B in the developing mammary gland results in abnormal terminal end buds (TEBs) that exhibit aberrant budding off the neck, histological anomalies, and a markedly thickened stroma. Overexpression of p190-B throughout postnatal development results in increased branching, delayed ductal elongation, and disorganization of the ductal tree. Interestingly, overexpression of p190-B during pregnancy results in hyperplastic lesions. Several cellular and molecular alterations detected within the aberrant TEBs may contribute to these phenotypes. Signaling through the IGF pathway is altered, and the myoepithelial cell layer is discontinuous at sites of aberrant budding. An increase in collagen and extensive infiltration of macrophages, which have recently been implicated in branching morphogenesis, is observed in the stroma surrounding the p190-B-overexpressing TEBs. We propose that the stromal response, disruption of the myoepithelial layer, and alterations in IGF signaling in the p190-B-overexpressing mice impact the TEB architecture, leading to disorganization and increased branching of the ductal tree. Moreover, we suggest that alterations in tissue architecture and the adjacent stroma as a consequence of p190-B overexpression during pregnancy leads to loss of growth control and the formation of hyperplasia. These data demonstrate that precise control of p190-B Rho GTPase-activating protein activity is critical for normal branching morphogenesis during mammary gland development. (*Molecular Endocrinology* 20: 1391–1405, 2006)

MAMMARY GLAND DUCTAL morphogenesis is a complex developmental process during which mammary epithelial cells must proliferate, migrate into the stromal fat pad, and differentiate into luminal and myoepithelial cell compartments (1). These processes occur within terminal end buds (TEBs), which drive the ductal penetration into the stromal fat pad (2). Ductal outgrowth is particularly dependent upon stromal-epithelial interactions, which provide proliferative and apoptotic cues as well as signals that effect cell migration (3, 4). Through their interactions with integrins, Rho GTP-binding proteins function to integrate extracellular signals to ultimately affect cell movement, proliferation, survival, and differentiation, all of which are essential events during ductal morphogenesis (5).

Precise regulation of Rho GTPase activity is critically important, and several families of proteins including the Rho GTPase-activating proteins (GAPs) are capable of modulating their activity (6). RhoGAPs function as negative regulators of Rho activity by enhancing the intrinsic GTPase activity of the Rho proteins to rapidly convert active GTP-bound Rho to inactive GDP-bound Rho (7). The role of the Rho-signaling pathway in mammary gland development and breast cancer progression is not well understood. Several studies have reported overexpression of Rho family members in human breast cancers (8–10), and a number of reports have delineated functions of the Rho pathway by introducing dominant-negative or active forms of Rho into breast cancer cell lines (11).

First Published Online February 9, 2006

Abbreviations: AKT, Protein kinase B; Dox, doxycycline; ECM, extracellular matrix; GAP, GTPase-activating protein; HA, hemagglutinin; H&E, hematoxylin and eosin; IGF-IR, IGF receptor I; IRES, interribosomal entry site; IRS, insulin receptor substrate; MTB, MMTV-rtTA transgenic mice; ROK, Rho kinase; RT, reverse transcriptase; rtTA, reverse tet transactivator; PAK, p21-activated kinase; pAKT, phosphorylate AKT; pPAK, phosphorylated PAK; pROK, phosphorylated ROK; TEB, terminal end bud; tet, tetracycline; TetO, tet operator.

***Molecular Endocrinology* is published monthly by The Endocrine Society (http://www.endo-society.org), the foremost professional society serving the endocrine community.**

Until recently, Rho signaling in normal mammary gland development had not been examined. P190-B RhoGAP, an important negative regulator of the Rho pathway, was identified in a screen for genes showing enriched expression in TEBs (12). P190-B is highly expressed throughout virgin mammary gland development in both the body and cap cell layers of the TEBs and in the mature ducts. Expression of p190-B decreases during late pregnancy and remains low, but detectable, during lactation. Homozygous deletion of this RhoGAP gene completely inhibits ductal outgrowth (12, 13). Loss of one allele of p190-B results in decreased proliferation within the TEBs, causing a transient delay in ductal morphogenesis. Thus, mammary gland development is critically dependent on p190-B RhoGAP.

To further elucidate the role of p190-B in mammary gland development and tumor progression, a tetracycline (tet)-regulatable p190-B-overexpressing mouse model was developed. This inducible system was chosen because it allows for manipulation of p190-B expression during distinct stages of mammary gland development and function. Using this approach, p190-B overexpression during ductal morphogenesis is shown to drastically alter TEB architecture. As a result, ductal elongation is delayed, branching is increased, and organization of the ductal tree is disrupted. Overexpression of p190-B during pregnancy results in hyperplastic lesions, which persist after postlactational involution. These studies demonstrate, for the first time, that overexpression of a RhoGAP is sufficient to disrupt mammary gland architecture and promote hyperplasia, confirming our previous findings that precise regulation of p190-B RhoGAP is critically important in the developing mammary gland.

RESULTS

P190-B Overexpression Results in Aberrant TEB Architecture

To generate the tet-regulatable p190-B-overexpressing mice, a transgene construct was designed in which a hemagglutinin (HA)-tagged human p190-B cDNA was subcloned into TMILA containing the tet operator (TetO)/minimal cytomegalovirus promoter elements followed by an interribosomal entry site (IRES)-luciferase (Fig. 1) (14). The presence of the IRES-luciferase allows for rapid identification of transgene expression in the mammary gland after induction. Injection of this construct into the pro-nuclei of fertilized FVB oocytes yielded nine founder lines, as determined by Southern blot and PCR analyses (Fig. 1 and data not shown).

To identify lines containing inducible p190-B transgene expression, bigenic mice were obtained by breeding the p190-B founder mice to mouse mammary tumor virus (MMTV)-rtTA (MTB) mice that express the reverse tet transactivator (rtTA) in the mammary epithelium under the control of the mouse MMTV long terminal repeat (Fig. 1A) (15). Bigenic mice (5 wk old) from each line and MTB control mice were treated with the tet analog doxycycline (Dox) at 2 mg/ml in their drinking water for 3–7 d to induce transgene expression. After treatment, mammary glands were dissected from the mice and analyzed for luciferase activity, p190-B transgene expression by RT-PCR, and morphological changes by whole-mount mammary gland analysis (Fig. 1C). Three of the lines (6667, 6671, and 6674, denoted with *asterisks* in Fig. 1B) showed inducible p190-B transgene expression as determined by luciferase activity and RT-PCR (Fig. 1, D and E). To determine which cell types express the p190-B transgene, immunofluorescence for the HA-tagged p190-B was performed on mammary gland tissue sections from Dox-treated midpregnant bigenic and MTB control mice. As expected, the HA-tagged p190-B transgene is localized to the mammary epithelial cells, which is consistent with the expression of the MMTV-rtTA within this compartment of the mammary gland (Fig. 1F) (15).

Because p190-B was originally identified in a screen for genes showing enriched expression in the TEBs, the effects of acute overexpression of p190-B on TEB morphology were examined. Strikingly, within 3 d of p190-B transgene induction, aberrant TEBs with extensive budding off the neck region were apparent in the whole-mounted mammary glands (Fig. 1C). Histological analysis of hematoxylin and eosin (H&E)-stained tissue sections from these glands further demonstrated the extent of disruption of the TEB architecture (Fig. 2, A and B). The TEBs exhibited extensive budding, abnormal morphologies, and disorganized and thickened stroma that, in some cases, encompassed the leading edge of the TEB. To quantify the extent of disruption of the TEB structures in the p190-B-overexpressing mice, the percentage of normal TEBs was determined after 3 d of transgene induction. Structures were designated normal if they did not exhibit budding off the neck region of the TEB. In comparison with the Dox-treated control mice ($n = 6$; 57 TEBs analyzed), the percentage of normal TEBs was significantly decreased in the p190-B-overexpressing mice [$n = 5$ (67 TEBs analyzed), 98.2 ± 1.85 *vs.* 34.8 ± 12.2 ($P < 0.0003$), respectively (Fig. 2E)]. Despite the pronounced TEB anomalies seen after short-term p190-B overexpression, acute overexpression of p190-B did not have any apparent effects on the morphology of the mature ducts in these mice (Fig. 2, C and D). These phenotypes were not observed in the Dox-treated MTB control mice. All three inducible lines showed the TEB phenotype, and subsequent studies were performed on two of the lines, 6667 and 6671. These results indicate that tight regulation of p190-B expression is critical to maintain normal TEB architecture.

P190-B overexpression is predicted to alter signaling downstream of Rho family proteins. One of the immediate downstream targets of the Rho-signaling pathway is Rho kinase (ROK). An increase in p190-B

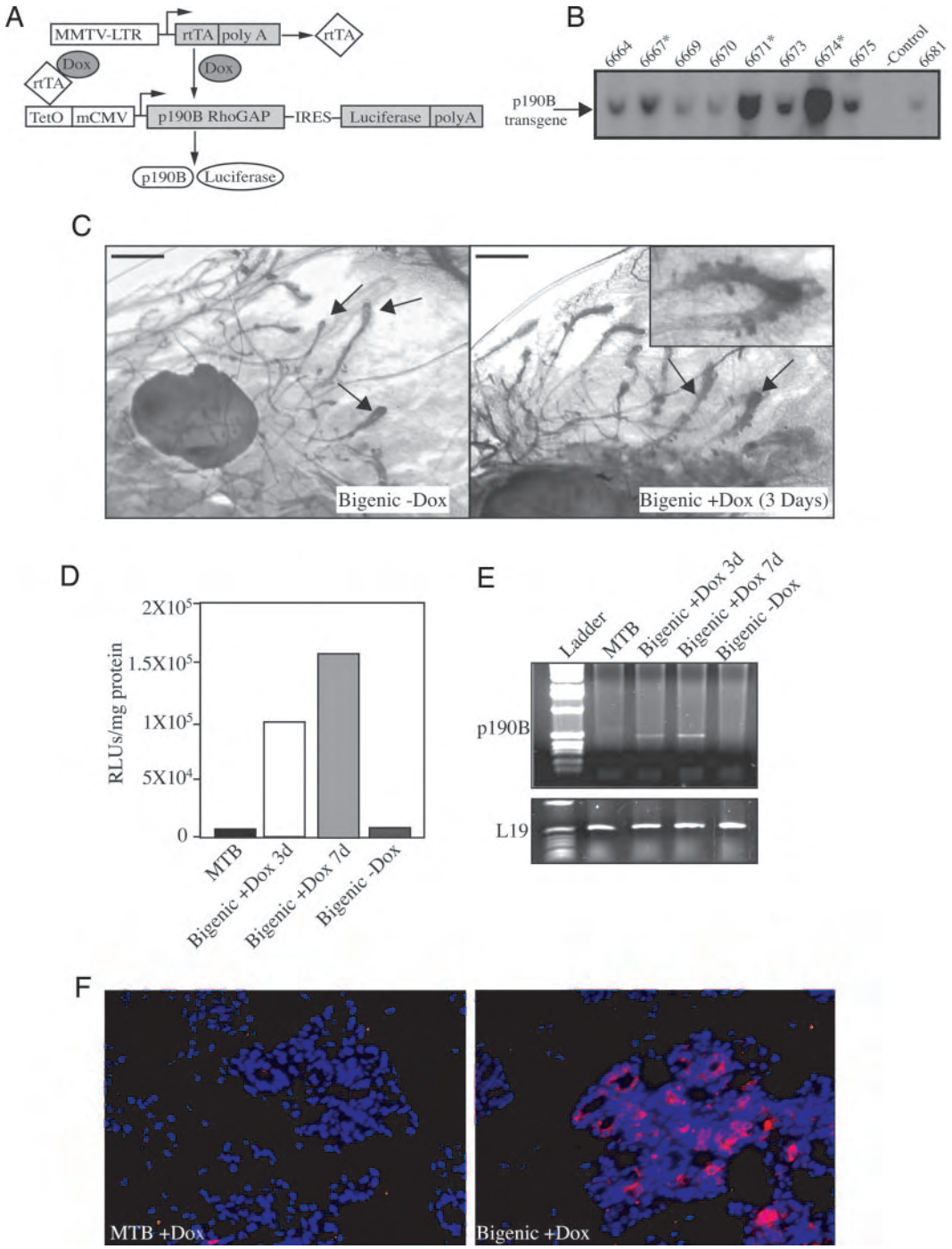

Fig. 1. Generation of Tet-Regulatable p190-B-Overexpressing Mice

A, A schematic of the two constructs used to generate bigenic tet-regulatable p190-B-overexpressing mice. B, Southern blot analysis of p190-B-overexpressing founder lines. *, Inducible lines. C, Whole-mount mammary glands showing aberrant budding off the neck region of p190-B-overexpressing TEBs compared with uninduced bigenic controls after 3 d of transgene induction. All three inducible lines showed this phenotype. Representative images at ×2.5 magnification are shown. *Bars*, 0.5 mm. D, Luciferase activity shown as relative light units (RLUs) per mg of protein in mammary glands from control and Dox-treated mice. E, RT-PCR analysis of p190-B transgene expression in mammary glands from control and Dox-induced mice. RT-PCR for L19 is shown as a control for the RT reaction. Reactions performed in the absence of RT did not contain products (data not shown). Data from line 6671 are presented in panels D and E and are representative of the three lines. F, Immunostaining for HA-tagged p190-B (*red*) on mammary gland tissue sections from d 18 pregnant mice demonstrates that transgene expression is localized to the mammary epithelial cells. Nuclei (*blue*) are 4′,6-diamidino-2-phenylindole stained. CMV, Cytomegalovirus; LTR, long terminal repeat.

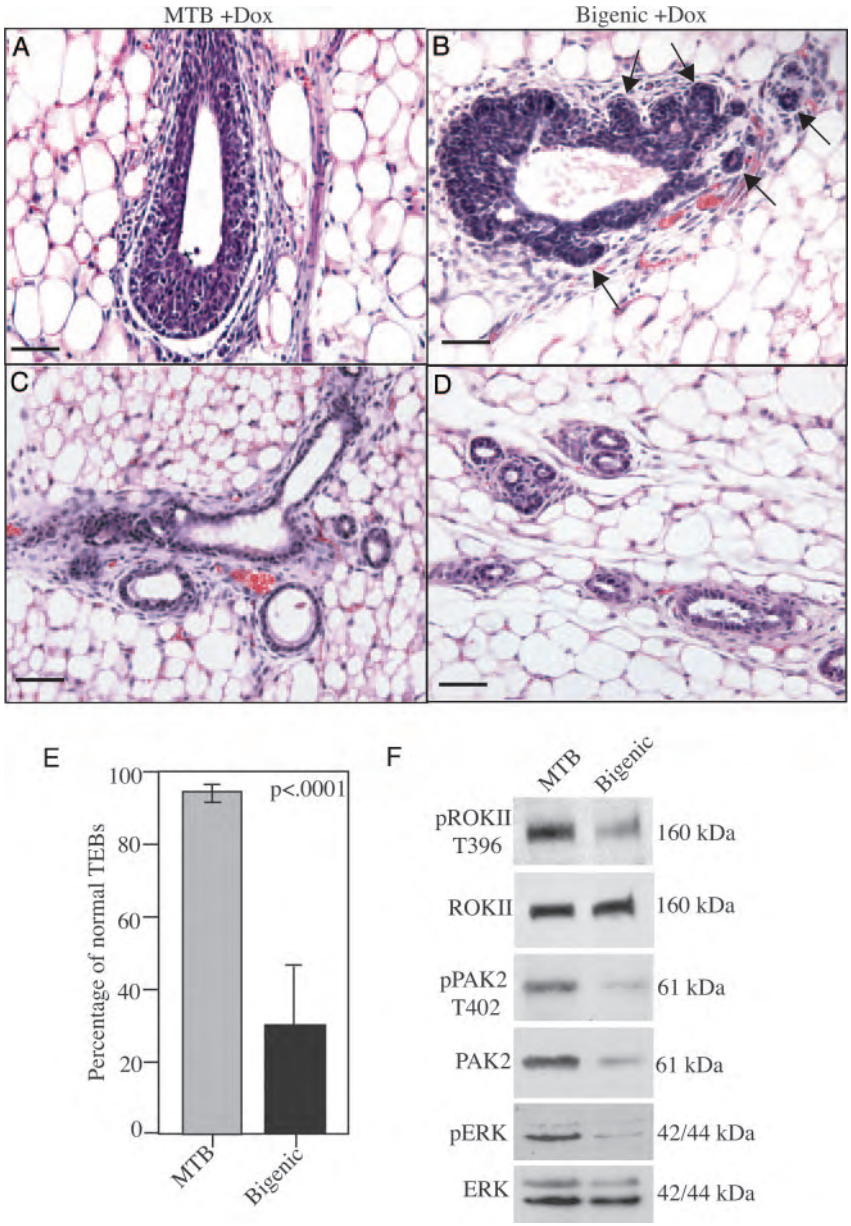

Fig. 2. p190-B Overexpression Disrupts TEB Architecture

Representative images of H&E-stained mammary gland tissue sections from bigenic or MTB control mice treated with Dox for 3 d are depicted. A, A TEB from a control mammary gland with normal architecture is shown. B, A TEB from a p190-B-overexpressing mammary gland with abnormal budding is shown (*arrows*). The mature ducts appear normal in the p190-B-overexpressing mice (panel D) as compared with the MTB control mice (panel C). *Scale bars*, 50 μm. E, The percentage of normal TEBs in p190-B-overexpressing (Bigenic) compared with control (MTB) mammary glands is depicted by a *graph*. F, Western analysis of phosphorylated and total ROKII, PAK-2, and ERK levels in p190-B-overexpressing and control mammary glands.

activity is expected to inhibit Rho activity and, consequently, decrease ROK activity. p190-B overexpression may also alter signaling downstream of the Rho family protein Rac, and p21-activated kinase (PAK) is one target of Rac that may be similarly down-regulated in response to p190-B overexpression. To examine whether this is the case, Western blotting for the phosphorylated active forms of ROKII (pROKII/Thr396) and PAK2 (pPAK2/Thr402) was performed. In comparison with the MTB control, pROKII expression was substantially diminished in the p190-B-overexpressing mammary glands (Fig. 2F). Total ROK expression, however, was equivalent between the MTB and p190-B-overexpressing mice. Similarly, pPAK-2 expression was lower, but this likely reflects decreased total PAK-2 expression that was detected in the p190-B-overexpressing as compared with the MTB control mammary glands (Fig. 2F). Recently, coordination of Rho and ERK signaling was shown to control tissue architecture (16). Thus, the pronounced decrease in

Rho signaling that was detected in the p190-B-overexpressing mammary glands might alter ERK activity. To investigate this possibility, Western blotting for phosphorylated ERK was performed. This analysis showed a marked decrease in phosphorylation of ERK, whereas total ERK levels were similar between the p190-B-overexpressing and MTB controls (Fig. 2F). Taken together, these results demonstrate that overexpression of p190-B in the mammary gland inhibits signaling downstream of the Rho family proteins.

To assess whether the newly formed buds off the neck region of the TEBs will persist or regress, cell proliferation and apoptosis were evaluated. To detect proliferation within the buds, immunohistochemical staining for the proliferation marker Ki67 was performed. As seen in Fig. 3B, the aberrant budding structures extending from the TEBs in the p190-B-overexpressing mice are highly proliferative. Apoptosis was assessed by immunohistochemical staining for the apoptotic marker, cleaved caspase-3, and few cells within the aberrant buds are undergoing apoptosis (Fig. 3D). These data suggest that the newly formed buds will grow out to form branches because the cells within the buds are proliferating and undergoing apoptosis similarly to cells within the control TEBs. Taken together, these data demonstrate that short-term p190-B overexpression disrupts TEB morphology and may lead to aberrant branching off of the neck of the TEB.

To further examine the morphological abnormalities seen in the p190-B-overexpressing TEBs, immunohistochemical staining was performed for cap/myoepithelial and body cell markers, p63 and E-cadherin, respectively (Fig. 3, E–H). This analysis demonstrated that both cell types are present within the aberrant TEBs. However, p63 immunostaining revealed that the cap/myoepithelial cell layer surrounding the aberrant TEBs is discontinuous along the neck region both at sites of aberrant budding and in areas not associated with aberrant budding (Fig. 3H). This disruption was not observed in the control TEBs, which show a continuous myoepithelial cell layer including at sites of initiating side branches distal to the TEBs (Fig. 3G, *arrowhead*; shown at higher magnification in the *inset*). Immunostaining for the myoepithelial marker smooth muscle actin also show discontinuity in this cell layer (data not shown). Thus, the alteration in the myoepithelial layer surrounding the abnormal TEBs does not appear to reflect a normal phenomenon associated with side branching. These data suggest that p190-B overexpression alters cell-cell or cell-extracellular matrix (ECM) interactions to impact the myoepithelial cell layer surrounding the TEBs.

P190-B Overexpression Results in Abnormal Stroma Surrounding the TEBs

Histological analysis of the H&E-stained TEBs demonstrated that the stroma surrounding the TEBs was altered in the p190-B-overexpressing mice. The stroma in the p190-B-overexpressing glands appeared disorganized, thicker, and more cellular. The degree of stromal disorganization correlated with the extent of TEB disruption such that the TEBs with drastically altered morphologies had more pronounced stromal anomalies. To further examine the stromal changes occurring in the p190-B-overexpressing mice, Masson's trichrome staining was performed as it allows for visualization of aniline blue-stained collagen fibers. As seen in Fig. 4B, the stroma surrounding the aberrant TEB from the p190-B-overexpressing mammary gland is highly enriched in collagen fibers as compared with the control TEB in which the collagen fibers are localized primarily to the neck region of the TEB (Fig. 4A). This result suggests that p190-B overexpression results in altered stromal-epithelial interactions during TEB outgrowth.

Immune cells, in particular macrophages and eosinophils, have recently been shown to play an important role in ductal morphogenesis in the developing mammary gland (17). Macrophages are also known to be involved in activation of stromal fibroblasts to affect ECM deposition (18). The aberrant budding off the TEBs, as well as the alterations in the stromal thickness and collagen deposition that were observed in the p190-B-overexpressing mice, suggested that there may also be alterations in immune cell infiltration surrounding the abnormal TEBs. To examine this possibility, immunohistochemical staining for the macrophage and eosinophil marker F4/80 was performed. In contrast to the control TEBs, which have fewer F4/80-positive cells localized predominantly to the neck region of the TEBs, the number of cells staining positive for F4/80 in the stroma surrounding the aberrant TEBs is markedly increased (Fig. 4, C and D). Taken together, these data suggest that p190-B overexpression influences immune cell infiltration within the stroma adjacent to the TEBs, which ultimately affects TEB architecture.

Downstream of p190-B RhoGAP are the insulin receptor substrate (IRS) proteins 1 and 2 (19). Deficiency of p190-B leads to increased ROK activity and phosphorylation of the IRS proteins, which targets them for degradation. As a result, IGF receptor (IGFR) signaling is diminished. Signaling through the IGFR pathway has also been shown to play an important role in mammary gland ductal morphogenesis because IGF-IR deficiency impairs take rate and ductal outgrowth in mammary gland transplantation studies (20). Constitutive activation of IGF-IR increases ductal side branching, delays ductal outgrowth, and results in rapid formation of adenocarcinomas (21). To determine whether signaling through the IGFR pathway is altered in the aberrant TEBs in the p190-B-overexpressing mice, immunohistochemistry for IRS-1, IRS-2, and a downstream target of the IGFR-signaling pathway, phosphorylated Akt (pAKT) was performed. Interestingly, this analysis revealed a reduction in IRS-1 and IRS-2 expression levels (Fig. 5, A–D) as well as a reduction in pAkt in the aberrant TEBs as compared with control

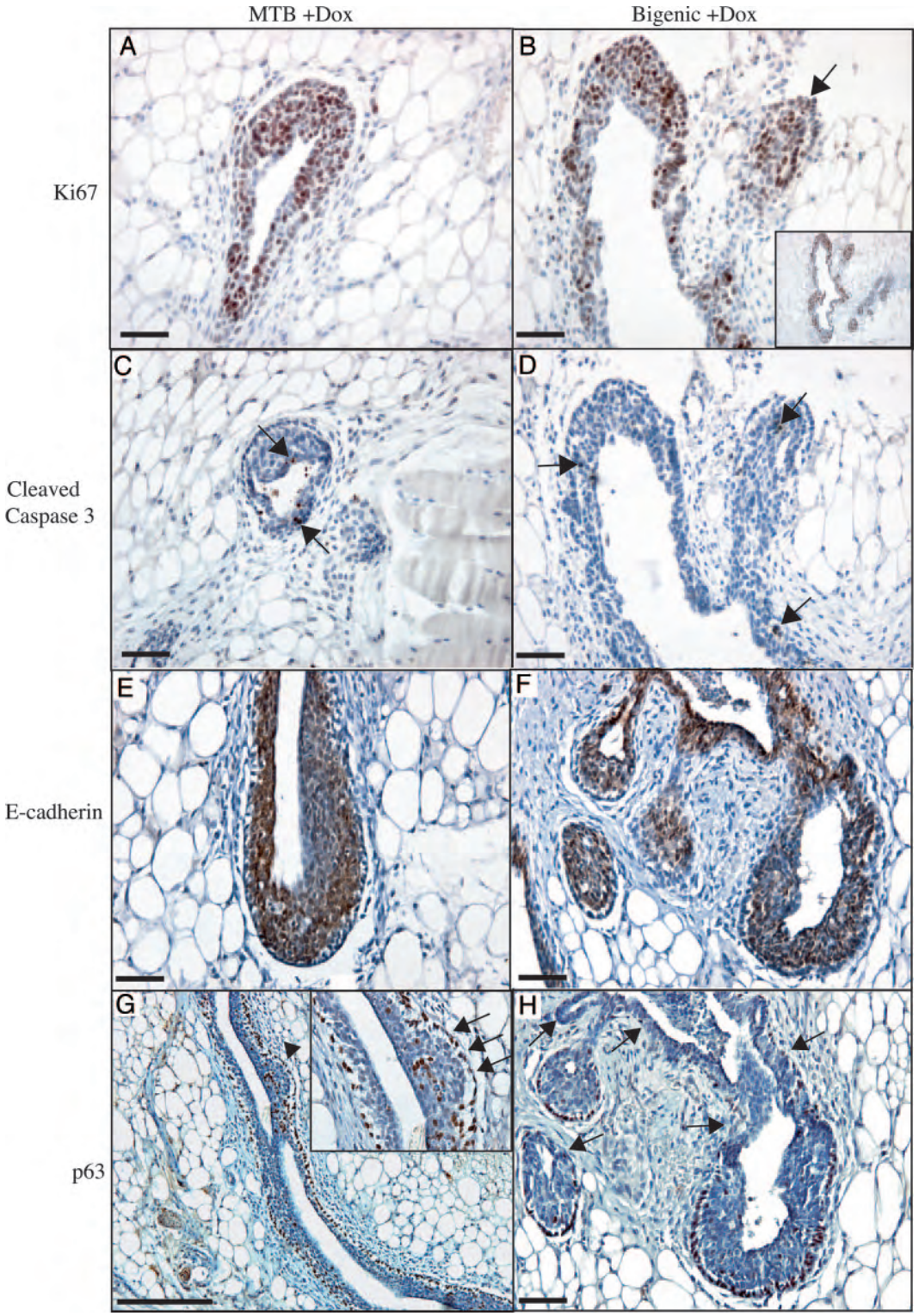

Fig. 3. Immunohistochemical Analysis of Proliferation, Apoptosis, and Cap/Myoepithelial and Body Cells in p190-B-Overexpressing TEBs

A and B, Immunostaining for the proliferation marker ki67 shows abundant proliferation in the control TEBs as well as the aberrant buds (*arrow*) in the p190-B-overexpressing TEBs. The *inset* shown in panel B demonstrates multiple buds extending from the TEB. C and D, Immunostaining for the apoptotic marker, cleaved caspase 3, shows that few cells are undergoing apoptosis in the abnormal buds similar to the control TEBs (*arrows* indicate positively stained cells). E and F, Immunostaining for E-cadherin marks the body cells in the TEBs. G and H, P63 immunostaining demonstrates noncontiguity of the myoepithelial cell layer in the p190-B-overexpressing TEBs (*arrows*) as compared with the control TEB, which shows a continuous cap/myoepithelial cell layer surrounding the TEB including at sites of side branching (*inset*, *arrows*). Note the thickened stroma surrounding the p190-B-overexpressing TEBs. *Scale bars*, 50 μm.

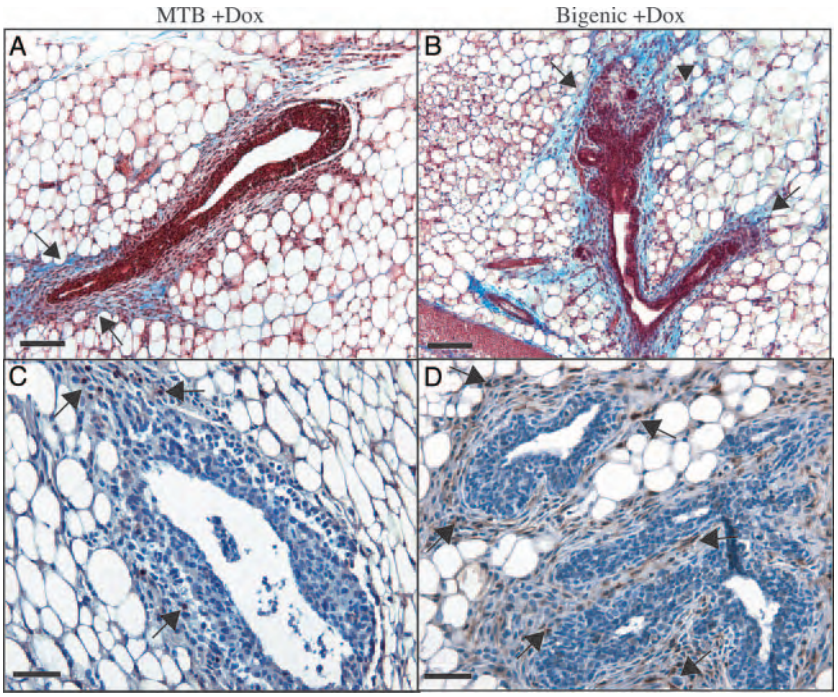

Fig. 4. Abnormal Stroma Surrounds p190-B-Overexpressing TEBs

A and B, Masson's trichrome staining shows increased collagen deposition (*arrows*, *blue area*) in the stroma surrounding the aberrant p190-B-overexpressing TEB as compared with the MTB control TEB. *Scale bars*, 100 μm. C and D, Immunostaining for the macrophage and eosinophil marker F4/80 shows abundant immune cells (*arrows*) within the stroma adjacent to the p190-B-overexpressing TEB as compared with the stroma surrounding the control TEB, which contains fewer immune cells that are localized primarily to the neck region of the TEB. *Scale bars*, 100 μm.

TEBs (Fig. 5, E and F). Western blotting of mammary gland extracts confirmed decreased expression of IRS-1, IRS-2, and total AKT in the p190-B-overexpressing as compared with the Dox-treated control mammary glands (Fig. 5G). Although a decrease in expression of these proteins in the aberrant TEBs was not predicted, these results indicate that p190-B overexpression impacts signaling through the IGFR pathway.

Long-Term p190-B Overexpression during Virgin Mammary Gland Development Results in Disorganization of the Ductal Tree

p190-B is normally highly expressed in the TEBs and mature ducts throughout postnatal mammary gland development. Acute overexpression (3–7 d) of p190-B resulted in pronounced abnormalities in the TEB architecture, including increased budding off the neck region of the TEBs. As shown in Fig. 3, analysis of proliferation and apoptosis within the aberrant TEBs suggested that these buds may persist and form new branches. To determine whether the TEB abnormalities would ultimately affect ductal outgrowth and formation of the arborized ductal tree, long-term p190-B overexpression studies were performed in which p190-B expression was induced throughout postnatal mammary gland development. For these studies, bigenic ($n = 6$; three mice from each line) and wild-type ($n = 4$) littermate control mice were treated continuously with Dox beginning at 5.5 wk of age until 9.5 wk of age, at which time the growing ducts normally reach the end of the fat pad. In comparison with the Dox-treated wild-type littermate control mammary glands, which showed normal architecture within the ductal tree, long-term p190-B overexpression resulted in disorganization of the ductal tree and increased branching, as seen in the whole-mounted mammary glands (Fig. 6B). Luciferase assays and RT-PCR were performed to confirm expression of the p190-B transgene (Fig. 6E and data not shown).

To quantify the increase in ductal branching, the average number of secondary and tertiary branch points was compared between the control and p190-B-overexpressing mice. This analysis revealed a significant increase in branching in the p190-B-overexpressing mice (21.9 ± 1.84 *vs.* 15.5 ± 1.93; $P < 0.03$) as compared with the control mice (Fig. 6F). Histological examination of H&E-stained tissue sections demonstrated that long-term p190-B overexpression throughout ductal morphogenesis results in the presence of abnormal TEBs and thickened stroma surrounding the mature ducts (Fig. 6, C and D). Normally at 9.5 wk of age, the TEBs have reached the end of the fat pad and begin to regress. TEBs were still detected in the most disorganized p190-B-overexpressing

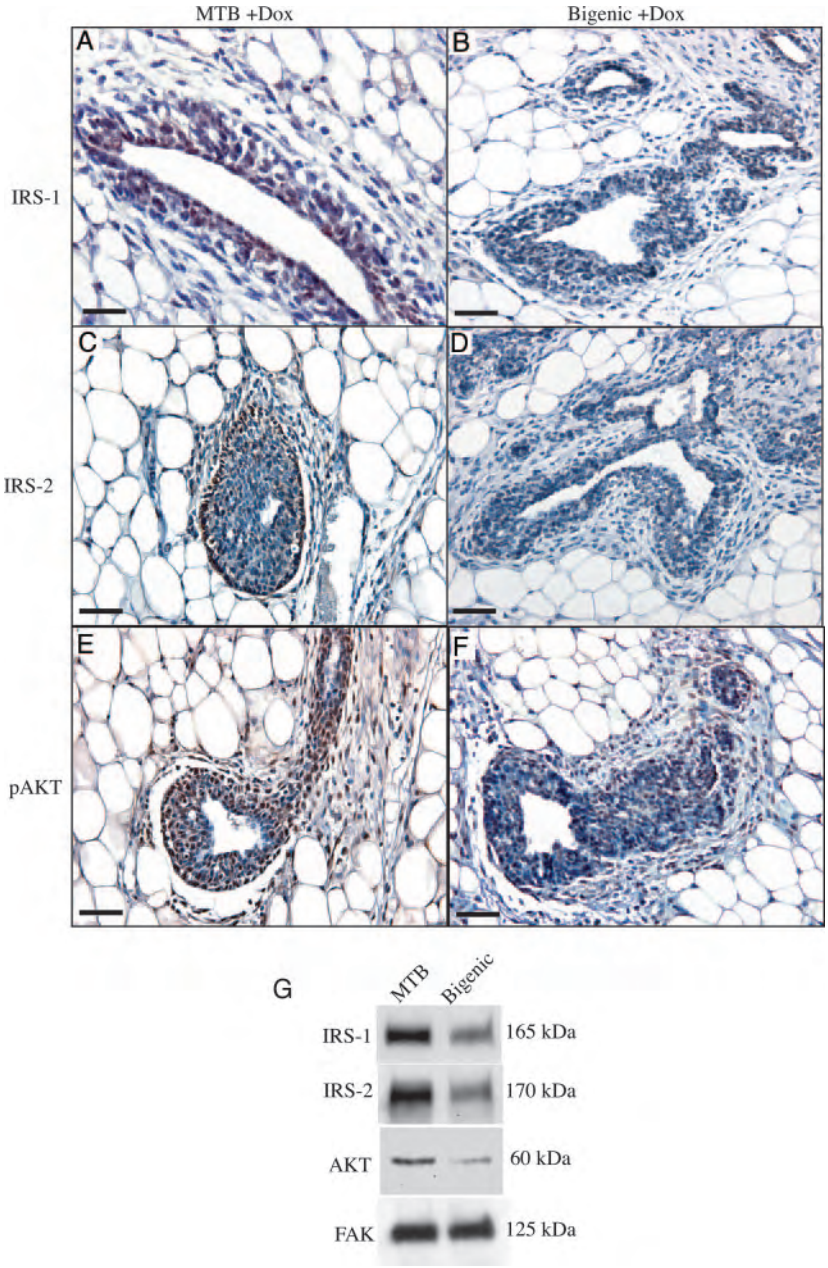

Fig. 5. Decreased IGFR Signaling in p190-B-Overexpressing TEBs

Immunohistochemical staining for IRS-1 (panels A and B), IRS-2 (panels C and D), and pAKT (panels E and F) demonstrated that expression of the IRS proteins and pAKT was significantly diminished in the aberrant p190-B-overexpressing TEBS as compared with control TEBs. *Scale bars*, 50 μm. G, Western blotting shows decreased IRS-1, IRS-2, and AKT expression in Dox-treated bigenic as compared with MTB control mammary glands. Focal adhesion kinase (FAK) is shown as a loading control.

mammary glands in which the ducts had not yet reached the end of the fat pad. Proliferation rates within the mature ducts were similar between the p190-B-overexpressing and Dox-treated wild-type littermate control mice as determined by quantification of Ki67-positive cells (2.6 $\pm$ 0.97 *vs.* 2.1$\pm$1.1; $P >$ 0.07). Taken together, these data demonstrate that the aberrant budding off the TEBs in the p190-B-overexpressing mice results in a disorganized ductal tree with increased branching and altered stroma surrounding the mature ducts.

Upon examination of the long-term p190-B-overexpressing mammary glands, it was noted that the severity of the aberrant branching and disorganization within the growing ductal tree correlated with a delay in ductal outgrowth. To further investigate the effects of p190-B overexpression on ductal elongation, p190-B-overexpressing mammary tissue was transplanted

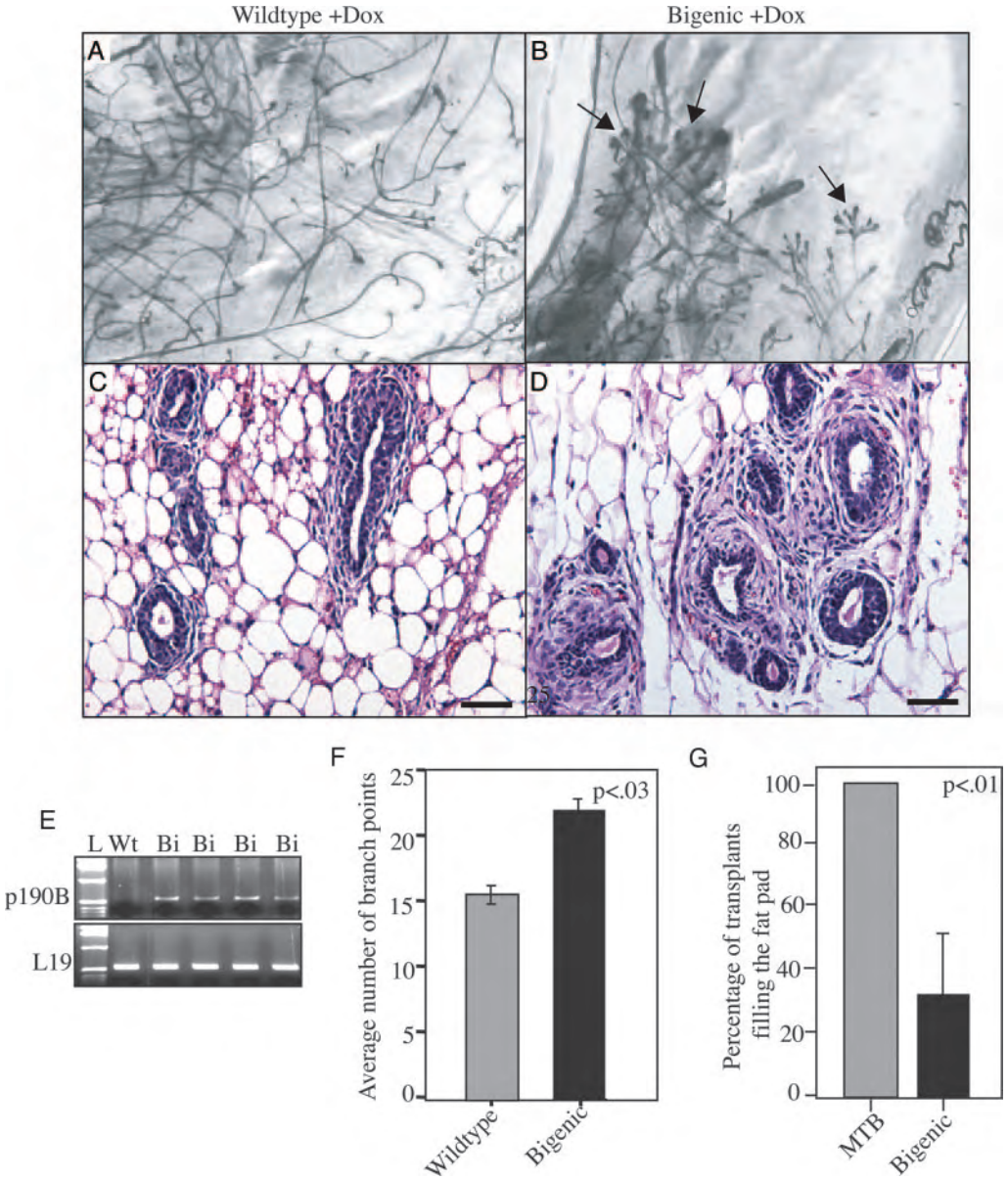

Fig. 6. Persistent Overexpression of p190-B during Ductal Morphogenesis Results in Delayed Ductal Elongation, Increased Branching, and Disorganization of the Ductal Tree

A and B, Whole-mounted mammary glands from Dox-treated wild-type control littermates and bigenic mice show aberrant architecture of the ductal tree in the p190-B-overexpressing mammary gland as compared with the normal ductal tree seen in the Dox-treated control. *Arrows* indicate the presence of abnormal TEBs. C and D, H&E-stained tissue sections show thickened stroma surrounding the ducts in the p190-B-overexpressing mammary glands as compared with the thin layer of connective tissue surrounding the ducts in the control mammary glands. *Scale bars*, 50 μm. E, RT-PCR shows p190-B transgene expression in the Dox-treated bigenic mice, but not in the wild-type controls. All wild-type controls were negative, and L19 and no-RT controls were performed (data not shown). F, Quantification of side branching in long-term Dox-treated mammary glands revealed a significant increase in the number of side branches in the p190-B-overexpressing mice compared with the Dox-treated wild-type control mice. The average number of branch points is shown by *graph*. G, The percentage of bigenic compared with MTB control transplants that filled the fat pad is shown by *graph*. Bi, Bigenic; Wt, wild type.

into the cleared fat pads of 3-wk-old female mice. As a control, MTB tissue was transplanted into the contralateral cleared no. 4 fat pads. The transplants were allowed to grow out for 8 wk, at which time the mice were bred to wild-type FVB males. Mammary glands were collected 3 d after parturition and analyzed by H&E staining. Luciferase assays were performed to confirm transgene expression (data not shown). Interestingly, p190-B overexpression resulted in a dramatic delay in ductal outgrowth as compared with the MTB

controls. This analysis revealed that 100% (six of six) of the MTB control transplants completely filled the fat pad, whereas only 33% (two of six) of the p190-B-overexpressing transplants filled the fat pad (n = 6; $P < 0.01$) (Fig. 6G). The remaining four p190-B-overexpressing transplants filled the fat pad 50% or less (data not shown). These data demonstrate that p190-B overexpression delays ductal morphogenesis, and pregnancy does not rescue this defect.

Overexpression of p190-B during Pregnancy Results in Hyperplastic Lesions

To examine the affects of p190-B overexpression during pregnancy and lactation, 12-wk-old bigenic (n = 6) and MTB (n = 3) and wild-type littermate (n = 3) control mice were bred to wild-type male mice. To induce p190-B transgene expression, Dox treatment was started when the males were placed with the females and continued throughout pregnancy and lactation. MTB and wild-type control mice were also Dox treated. During late pregnancy (d 16–18) 3- to 5-mm biopsy samples were collected from the bigenic (n = 2) and wild-type littermate (n =2) control mice. Interestingly, histological examination of H&E-stained sections of biopsy samples from both bigenic mice showed hyperplastic lesions that were readily detectable within the small samples that were collected (Fig. 7, C and D). Neither of the wild-type controls contained hyperplastic lesions. Furthermore, hyperplastic lesions were detected in involuted mammary glands from the p190-B-overexpressing mice, but not in the controls (Fig. 7B). Overexpression of p190-B, however, did not inhibit lactation because all six bigenic mice were able to support their litters (six or more pups) to weaning age.

DISCUSSION

Reported here for the first time is an *in vivo* model in which the effects of tet-regulatable p190-B RhoGAP overexpression on mammary gland development and function are examined. To date, investigation of the role of the Rho pathway in the mammary gland has been performed primarily in breast cancer cell lines in which Rho signaling is manipulated by overexpression of either dominant-active or inhibitory forms of Rho (11). More recently, small interfering RNA has been used to down-regulate specific Rho family members in breast cancer cell lines (22, 23). These studies have elucidated roles for the Rho-signaling pathway in proliferation, adhesion, and invasion of breast cancer cells. However, they have not allowed for examination of this pathway in normal mammary epithelial cells in the context of the *in vivo* environment, which includes stromal-epithelial interactions that are critical for mammary gland development, function, and breast cancer progression. In the current study, the p190-B transgene is under the control of a tet-regulatable promoter, which provides temporal control allowing for investigation of the effects of overexpression of this

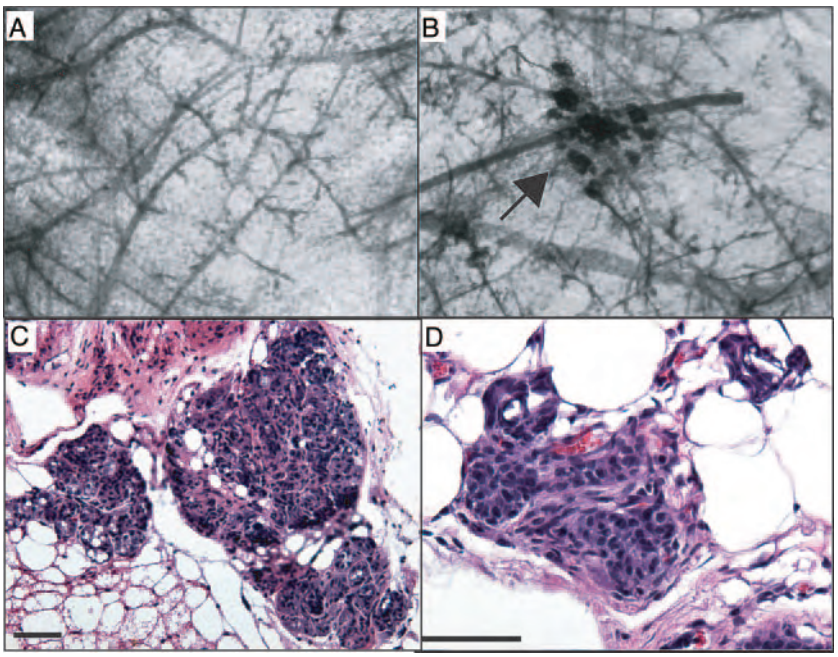

Fig. 7. p190-B Overexpression during Pregnancy Results in Hyperplastic Lesions

A and B, Hyperplastic lesions from p190-B-overexpressing mice are shown in whole-mounted involuted mammary glands (panel B, *arrow*), whereas no lesions were detected in the Dox-treated MTB control glands (panel A). Magnification, ×4. C and D, H&E-stained sections showing the histology of the hyperplastic lesions from each biopsy. *Scale bars*, 50 μm.

RhoGAP at distinct stages of mammary gland development and function. This unique aspect allowed us to examine the effects of p190-B overexpression on ductal outgrowth in the developing virgin and during pregnancy and lactation.

Acute overexpression of p190-B during ductal morphogenesis dramatically altered the architecture of the TEBs and the adjacent microenvironment. The abnormal TEBs were characterized by extensive budding off the neck region, disruption of the myoepithelial cell layer, and pronounced stromal alterations. Overexpression of p190-B throughout ductal morphogenesis resulted in delayed ductal elongation, disorganization of the ductal tree, and increased side branching. Previously, loss of p190-B was shown to completely inhibit ductal morphogenesis (13). Haploinsufficiency of p190-B was shown to transiently delay ductal morphogenesis, due to decreased proliferation in the cap cell layer of the TEB, possibly resulting from diminished expression of IRS proteins (13). The current study complements the loss of function studies and demonstrates that precise regulation of p190-B in the developing mammary gland is required for normal TEB structure, ductal elongation, and organization of the ductal tree.

p190-B overexpression resulted in several cellular and molecular changes within the TEBs and surrounding microenvironment, all of which are likely to contribute to the aberrant TEB architecture. Interestingly, the myoepithelial layer was found to be discontinuous along the neck region and at sites of aberrant budding in the p190-B-overexpressing TEBs. In contrast, alterations in the myoepithelial cell layer were not detected at sites of lateral budding or at any point along the neck region of the control TEBs. This result suggests that disruption of the myoepithelial cell layer in the aberrant TEBs is not reflective of a normal phenomenon associated with lateral branch points. However, the role of the myoepithelial cell layer in the formation of lateral branches is not clear. One model in the literature suggests that the myoepithelial cell layer is normally absent at branch points, although the data supporting this model are unclear (24). In contrast to this model, it has also been suggested that the myoepithelial cells reform the cap cell layer during the initiation of lateral branches (25). One possible role for the myoepithelial cells, which secrete a number of proteases, is that they may contribute to maintenance and remodeling of the ECM underlying the ductal epithelium during lateral branching (26). Furthermore, myoepithelial cells may have tumor suppressor roles because they have been shown to inhibit proliferation, induce apoptosis, and block invasion of breast cancer cells (27–29). Mice overexpressing an inducible form of fibroblast growth factor receptor 1 (MMTV-iFGFR1) also had a noncontiguous myoepithelial cell layer at sites of aberrant branching (30). Thus, disruption of the myoepithelial cell layer in the p190-B-overexpressing TEBs may play an important role in the abnormal TEB architecture and aberrant budding off the neck region of the TEBs. The molecular mechanisms by which overexpression of p190-B contributes to alterations in the myoepithelial cell layer remain unclear. Future studies examining the interactions between primary myoepithelial and luminal epithelial cells isolated from the tet-regulatable p190-B-overexpressing mice in a three-dimensional culture system will help to elucidate the molecular signaling pathways involved in the cross-talk between the myoepithelial and luminal epithelial cells.

Another phenotype observed in the aberrant TEBs was a pronounced alteration in the adjacent microenvironment. The stroma was thicker, more cellular, and contained more collagen as determined by Masson's trichrome staining. Recently, elegant studies by Dr. Valerie Weaver and colleagues (16) demonstrated that matrix rigidity plays a critical role in epithelial morphogenesis. Rho-dependent cytoskeletal tension and ERK activity are increased in epithelial cells grown on a stiff stroma, thereby altering cell-cell/cell-matrix adhesion and polarity to ultimately disrupt morphogenesis. These studies demonstrated that even small increases in matrix stiffness are sufficient to increase cell proliferation and compromise tissue architecture. Furthermore, ROK-mediated contractility is required for breast epithelial cells to sense the rigidity of their environment, and down-regulation of Rho activity is necessary for epithelial cell differentiation (31). Thus, the increase in collagen and stromal thickness adjacent to the aberrant TEBs may result in a more rigid stroma, leading to disrupted TEB architecture in the p190-B-overexpressing mice.

Interestingly, ROK and PAK activity is decreased in the p190-B-overexpressing mammary glands. The Rho pathway plays an essential role in regulation of actin cytoskeletal dynamics, and remodeling of the actin cytoskeleton is required for a number of cellular processes (32). Continual inhibition of Rho signaling by overexpression of p190-B RhoGAP, therefore, is not likely to be tolerated within normal mammary epithelial cells. Thus, it is probable that a compensatory up-regulation of other signaling pathways that contribute to cytoskeletal regulation occurs in response to p190-B overexpression. The stromal response in the p190-B-overexpressing mice may occur to compensate for the chronically depressed ROK and PAK activity, thereby allowing for modulation of Rho-dependent cytoskeletal tension.

In addition to the changes in matrix deposition, a significant increase in the number of immune cells was detected by immunostaining for the macrophage and eosinophil marker F4/80. Whereas disruption of the myoepithelial cell layer may contribute to alterations in the stromal environment as discussed above, it is likely that p190-B overexpression modulates inside-out signaling pathways that influence immune cell infiltration and ECM deposition. Macrophages and eosinophils have been shown to play an essential role in branching morphogenesis of the mammary gland because depletion of these cells inhibited ductal branch-

ing and elongation (17). Their ability to promote ECM remodeling and aid in the release of growth factors may contribute to the disruption in ductal morphogenesis seen in the p190-B-overexpressing mice. Thus, the aberrant budding off the TEBs and increased branching observed after long-term p190-B overexpression is likely to be influenced by the marked increase in F4/80-positive immune cells observed in association with the aberrant TEBs. The molecular mechanisms by which overexpression of p190-B contributes to the recruitment of immune cells remain unclear. In breast cancer cells, the Rho-signaling pathway was shown recently to be important for production of colony-stimulating factor 1 (33), which is a major regulator of macrophage activation (34). Thus, it is possible that p190-B overexpression leads to alterations in Rho signaling that impact expression of colony-stimulating factor 1 expression, resulting in the recruitment of macrophages.

Similar to p190-B RhoGAP, IGF-IR is critical for normal mammary gland ductal morphogenesis. In transplant studies, embryonic mammary buds deficient for IGF-IR show a significant reduction in take rate, and ductal outgrowth is severely impaired (20). Overexpression of a constitutively active IGF-IR in the developing mammary gland increased side branching, delayed ductal elongation, and resulted in the rapid formation of adenocarcinomas (21). p190-B RhoGAP was recently shown to interact with the IGF-signaling axis *in vivo*. Deficiency of p190-B resulted in increased activity of ROK, which phosphorylates the IRS proteins and targets them for degradation (19). In addition, IGF-IR activation positively regulates p190-B activity through phosphorylation events that alter the subcellular location of p190-B (35). Furthermore, decreased expression of IRS-1 and IRS-2 was detected in the TEBs of p190-B heterozygous mice (13). Thus, interactions between IGF-IR and p190-B signaling are likely to play an important role in the developing mammary gland.

In the current report, expression of the IRS proteins and activation of the downstream effector AKT were significantly reduced in the aberrant TEBs. This result was initially unexpected because p190-B deficiency also results in reduced IGFR signaling. Although it may seem surprising that IGFR signaling is decreased as a result of both p190-B deficiency and overexpression, this finding may not be unexpected when considering that normal regulation of Rho signaling is highly dynamic (32). Chronic suppression of a pathway that normally undergoes transient fluctuations may have unanticipated effects on interacting pathways. Furthermore, overexpression of p190-B should not necessarily lead to an increase in IRS-1/2 expression just because the reciprocal experiment was shown to lead to increased ROK activity and IRS degradation (19). There may be a finite level of IRS gene expression, and the steady-state level does not, therefore, necessarily have to increase when p190-B is overexpressed. The reduced IGFR signaling in response to p190-B overexpression may account for the delayed ductal elongation that was detected in the p190-B-overexpressing mice, whereas the increased branching may result from changes in the stromal compartment and cap/myoepithelial cell layer as discussed above.

The ability to temporally regulate expression of the p190-B transgene allowed for examination of the role of p190-B overexpression during distinct stages of mammary gland development and function. To investigate the consequences of p190-B overexpression during pregnancy and lactation, the transgene was induced on the first day of pregnancy and continued throughout lactation. p190-B overexpression did not have any apparent effect on lactation. Interestingly, hyperplastic lesions were detected in biopsies from p190-B-overexpressing pregnant and involuted mammary glands. To our knowledge, this is the first report in which overexpression of a RhoGAP was shown to have neoplastic activities *in vivo*. One potential explanation for the development of these lesions is that there may also be perturbations in the myoepithelial cell layer when p190-B is overexpressed during pregnancy, which could lead to a loss of growth control as discussed above. Alternatively, increased rigidity of the stroma may lead to loss of growth control and tissue architecture (16). Analysis of multiparous mice in which p190-B is chronically overexpressed is necessary to determine whether these hyperplastic lesions will progress. This study, as well as transplantation of the hyperplastic lesions, is currently ongoing.

MATERIALS AND METHODS

Transgenic Mice

To generate the tet-regulatable p190-B transgenic mice, the following construct was engineered. The 4.9-kb human p190-B cDNA was subcloned into the TMILA TetO-IRES-luciferase vector downstream of the TetO (14). A 7.2-kb fragment containing the TetO-p190-B-IRES-luciferase expression cassette was microinjected into the pronuclei of fertilized FVB/N oocytes by the Baylor College of Medicine Transgenic Mouse Core, yielding nine potential founder lines. Southern blotting to detect the transgene in genomic DNA prepared from tail cuts was performed to identify founder lines. Mice were maintained on an inbred FVB/N background.

Bigenic mice were obtained by breeding TetO-p190-B-IRES-luciferase mice to MTB mice, which contain the reverse tet transactivator under the control of the MMTV promoter (15). For genotyping, PCR amplification of the MTB and p190-B transgenes was performed on genomic DNA prepared from tail cuts using the following oligonucleotide pairs: for TetO-p190-B, 5′-CCTCAAAAAAGTCATGGGGAACG-GAGC-3′ and 5′-CGCTGACACGGTAGAGTCCTTCGG-3′; for MTB, 5′-TCCAAGGGCATCGGTAAACA-3′ and 5′-GCAT-CAAGTCGCTAAAGAAG-3′. The p190-B oligonucleotide pair is specific for the human p190-B transgene and does not cross-react with endogenous murine p190-B. Reaction conditions were 94 C for 3 min followed by 30 cycles of 94 C for 30 sec, 60 C for 45 sec, 72 C for 45 sec, followed by a 5-min extension at 72 C. To induce transgene expression, bigenic mice were treated with Dox (CLONTECH, Mountain View, CA) at 2 mg/ml in their drinking water containing 5% sucrose. Fresh Dox water was given twice weekly. Animal care and

procedures were approved by the Institutional Animal Care and Use committee at Baylor College of Medicine and were in accordance with the procedures outlined in the Guide for Care and Use of Laboratory Animals (National Institutes of Health publication 85–23).

For mammary gland transplantation, the inguinal no. 4 mammary glands from 21-d-old FVB/N female mice were cleared of the mammary epithelium as previously described (36). Small pieces of tissue approximately 1 mm (3) in size were transplanted into the cleared fat pads. Transplants were allowed to grow out for 8 wk. Mammary gland tissue isolation and whole-mount preparation were performed as previously described (37). Analysis of branch points and TEB morphology were performed blindly by examining whole-mounted mammary glands. For branch point analysis, the primary duct was identified starting at the nipple, and the average number of secondary and tertiary branch points off the primary duct was determined. The unpaired Student's *t* test was used to determine statistical significance.

Luciferase Assay

Snap-frozen mammary tissue was ground using a mortar and pestle. Tissue extracts were prepared in Passive Lysis Buffer (Promega Corp., Madison, WI) and cleared by centrifugation. Luciferase activity was measured using Promega's Luciferase Assay System according to the manufacturer's instructions. Protein concentrations in the tissue extracts were determined using the BCA Protein Quantitation Assay (Pierce Chemical Co., Rockford, IL).

Southern Hybridization

A random primed (DNA labeling kit, Roche, Indianapolis IN) cDNA probe recognizing the first 1.3 kb of the human p190-B coding region was used to probe Southern blots containing *Eco*RI-digested genomic DNA prepared from tail cuts as previously described (38). The digested DNA was transferred to Zetaprobe (Bio-Rad Laboratories, Inc., Hercules, CA).

Immunohistochemical Staining

Paraffin-embedded tissue sections (5 μm) were deparaffinized in xylenes and rehydrated through a series of graded ethanols. Tissue sections were then stained with hematoxylin and eosin, Accustain (Masson's) Trichrome stain (Sigma-Aldrich, St. Louis, MO), or antibodies to detect specific proteins. Antigen retrieval was performed by microwaving slides in 10 mM citrate, pH 6, for 20 min. For immunostaining with mouse monoclonal antibodies, the M.O.M kit (Vector Laboratories, Burlingame, CA) was used to block nonspecific binding and for dilution of primary antibodies. For primary polyclonal antibodies, the tissue sections were blocked and primary antibodies were diluted in a 5% solution of BSA in PBS + 0.5% Tween-20. Sections were incubated with primary antibody overnight at room temperature. The following antibodies and dilutions were used: E-cadherin, 1:250 (BD Transduction Laboratories, San Jose, CA); Ki67, 1:5000 (Santa Cruz Biotechnology, Inc., Santa Cruz, CA); cleaved caspase-3 (Asp175), 1:1000 (Cell Signaling, Beverly MA); p63, 1:500 (Lab Vision Neomarkers, Fremont, CA); IRS-1, 1:800 (Upstate Biotechnology, Inc., Lake Placid, NY); IRS-2 1:800 (Upstate Biotechnology); pAKT (Ser473), 1:50 (Cell Signaling); F4/80, 1:50 with no antigen retrieval (Caltag Laboratories, Burlingame, CA). Biotinylated antirat (Molecular Probes, Eugene, OR), antirabbit (Oncogene Research, Darmstadt, Germany), and antimouse (Oncogene Research) secondary antibodies were diluted 1:200 in PBS and were incubated on the tissue sections for 1 h at room temperature. Vectastain Elite ABC and diaminobenzidine substrate kits were used to detect immunoperoxidase staining according to the manufacturer's instructions (Vector Laboratories). To detect the HA-tagged p190-B by immunofluorescence, tissue sections from 18-d pregnant mice were subjected to antigen retrieval as described above. To detect the HA tag, a monoclonal antibody against HA 1:200 (Covance Laboratories, Inc., Denver, PA) was used with the M.O.M kit. Fluorescent-tagged antimouse Alexa 594 secondary antibody (Molecular Probes) was used at 1:1000. Nuclei were visualized by staining with 4′,6-diamidino-2-phenylindole.

RT-PCR

RNA was prepared from mammary glands using Trizol Reagent according to the manufacturer's recommendations. To prepare cDNA, 1 μg of RNA was first DNase treated, primed with oligo-dT, and reverse transcribed using MMLV-reverse transcriptase (RT) (all reagents for RT were purchased from Invitrogen, Carlsbad CA). The human p190-B-specific oligonucleotides that were used for genotyping PCR were also used for RT-PCR. As a negative control, reactions were also performed in the absence of RT (data not shown). Amplification of L19 served as a control for the RT reaction. The following oligonucleotides and conditions were used: 5′-AGTATCCTCAGGCTTCAGAA-3′ and 5′-TTCCTTGGTCTTAGACCTGC-3′. Reaction conditions were 94 C for 3 min followed by 30 cycles of 94 C for 30 sec, 60 C for 45 sec, 72 C for 45 sec, followed by 5 min at 72 C.

Western Blotting

To examine expression and phosphorylation of proteins by Western analysis, mammary gland extracts were first prepared by pulverizing snap-frozen tissues followed by lysis in Passive Lysis Buffer (Promega) containing a protease inhibitor cocktail (Roche) and clearing by centrifugation. Protein concentrations in the tissue extracts were determined using the BCA Protein Quantitation Assay (Pierce). Mammary gland extracts were prepared from p190-B-overexpressing (n = 4) or MTB control glands (n = 4) at d 3 of involution that had been treated continuously with Dox throughout pregnancy and involution. Extracts were pooled (20 μg of each), electrophoresed on 6% or 12% SDS-PAGE gels, and transferred to polyvinylidine difluoride membrane (Millipore Corp., Bedford MA). Membranes were blocked in 5% milk/Tris-buffered saline followed by incubation with pROKII (thr396) 1:1000 or total ROKII 1:1000 antibodies (AnaSpec, Inc., San Jose, CA), IRS-1 and IRS-2 1:1000 (Upstate Biotechnology), AKT 1:1000 (Cell Signaling), pPAK-2 (thr402) and total PAK-2 1:1000 (Cell Signaling), focal adhesion kinase 1:1000 (Cell Signaling), and phosphorylated ERK and ERK 1:1000 (Cell Signaling) in 5% milk/Tris-buffered saline-Tween 20. Peroxidase-conjugated goat antirabbit secondary antibody (Jackson ImmunoResearch Laboratories, Inc., West Grove, PA) was used at 1:5000, and signal was detected with Supersignal West Pico Solutions (Pierce). Membranes were stripped and reprobed whenever possible. Fast green stain was also used to confirm equal loading of proteins on the membranes (data not shown).

Acknowledgments

We thank Shirley Small for her help with animal husbandry and colony management; Maria Gonzalez-Rimbau for technical support; and Mercy Chen for assistance with mammary gland transplantation.

Received October 25, 2005. Accepted February 2, 2006.

Address all correspondence and requests for reprints to: Jeffrey M. Rosen, Ph.D., C.C. Bell Professor of Molecular and

Cellular Biology and Medicine, DeBakey Building, M638a, Baylor College of Medicine, One Baylor Plaza, Houston, Texas 77030-3498. E-mail: jrosen@bcm.tmc.edu.

This work was supported by National Institutes of Health Grant CA030195-22 and by a postdoctoral fellowship (DAMD17-03-1-0325) from the Department of Defense Breast Cancer Research Program (to T.V.-G.).

Disclosure summary: T.V-G., B.H., E.G., and J.R. have nothing to declare. L.C. has received lecture fees from Amgen, Inc., Bristol-Meyers Squibb, Merck & Co., Inc., Eli Lilly & Co., and Genentech, Inc.

REFERENCES

1. Bissell MJHH 1987 Form and function in the mammary gland: the role of extracellular matrix. New York: Plenum Publishing Corp.
2. Hinck LaS, Gary B 2005 The mammary end bud as a motile organ. Breast Cancer Res 7:245–251
3. Fata JE, Werb Z, Bissell MJ 2004 Regulation of mammary gland branching morphogenesis by the extracellular matrix and its remodeling enzymes. Breast Cancer Res 6:1–11
4. Parmar H, Cunha GR 2004 Epithelial-stromal interactions in the mouse and human mammary gland in vivo. Endocr Relat Cancer 11:437–458
5. Karnoub AE, Symons M, Campbell SL, Der CJ 2004 Molecular basis for Rho GTPase signaling specificity. Breast Cancer Res Treat 84:61–71
6. Lin M, van Golen KL 2004 Rho-regulatory proteins in breast cancer cell motility and invasion. Breast Cancer Res Treat 84:49–60
7. Burbelo PD, Miyamoto S, Utani A, Brill S, Yamada KM, Hall A, Yamada Y 1995 p190-B, a new member of the Rho GAP family, and Rho are induced to cluster after integrin cross-linking. J Biol Chem 270:30919–30926
8. Rihet S, Vielh P, Camonis J, Goud B, Chevillard S, de Gunzburg J 2001 Mutation status of genes encoding RhoA, Rac1, and Cdc42 GTPases in a panel of invasive human colorectal and breast tumors. J Cancer Res Clin Oncol 127:733–738
9. van Golen KL, Davies S, Wu ZF, Wang Y, Bucana CD, Root H, Chandrasekharappa S, Strawderman M, Ethier SP, Merajver SD 1999 A novel putative low-affinity insulin-like growth factor-binding protein, LIBC (lost in inflammatory breast cancer), and RhoC GTPase correlate with the inflammatory breast cancer phenotype. Clin Cancer Res 5:2511–2519
10. Fritz G, Just I, Kaina B 1999 Rho GTPases are overexpressed in human tumors. Int J Cancer 81:682–687
11. Burbelo P, Wellstein A, Pestell RG 2004 Altered Rho GTPase signaling pathways in breast cancer cells. Breast Cancer Res Treat 84:43–48
12. Chakravarty G, Roy D, Gonzales M, Gay J, Contreras A, Rosen JM 2000 P190-B, a Rho-GTPase-activating protein, is differentially expressed in terminal end buds and breast cancer. Cell Growth Differ 2000 11:343–354
13. Chakravarty G, Hadsell D, Buitrago W, Settleman J, Rosen JM 2003 p190-B RhoGAP regulates mammary ductal morphogenesis. Mol Endocrinol 17:1054–1065
14. Gunther EJ, Moody SE, Belka GK, Hahn KT, Innocent N, Dugan KD, Cardiff RD, Chodosh LA 2003 Impact of p53 loss on reversal and recurrence of conditional Wnt-induced tumorigenesis. Genes Dev 17:488–501
15. Gunther EJ, Belka GK, Wertheim GB, Wang J, Hartman JL, Boxer RB, Chodosh LA 2002 A novel doxycycline-inducible system for the transgenic analysis of mammary gland biology. FASEB J 16:283–292
16. Paszek MJ, Zahir N, Johnson KR, Lakins JN, Rozenberg GI, Gefen A, Reinhart-King CA, Margulies SS, Dembo M, Boettiger D, Hammer DA, Weaver VM 2005 Tensional homeostasis and the malignant phenotype. Cancer Cell 8:241–254
17. Gouon-Evans V, Rothenberg ME, Pollard JW 2000 Postnatal mammary gland development requires macrophages and eosinophils. Development 127:2269–2282
18. Song E, Ouyang N, Horbelt M, Antus B, Wang M, Exton MS 2000 Influence of alternatively and classically activated macrophages on fibrogenic activities of human fibroblasts. Cell Immunol 204:19–28
19. Sordella R, Classon M, Hu K-Q, Matheson SF, Brouns MR, Fine F, Zhang L, Takami H, Yamada Y, Settleman J 2002 Modulation of CREB activity by the Rho GTPase determines cell size during embryonic development. Dev Cell 2:553–565
20. Bonnette SG, Hadsell DL 2001 Targeted disruption of the IGF-I receptor gene decreases cellular proliferation in mammary terminal end buds. Endocrinology 142: 4937–4945
21. Carboni JM, Lee AV, Hadsell DL, Rowley BR, Lee FY, Bol DK, Camuso AE, Gottardis M, Greer AF, Ho CP, Hurlburt W, Li A, Saulnier M, Velaparthi U, Wang C, Wen ML, Westhouse RA, Wittman M, Zimmermann K, Rupnow BA, Wong TW 2005 Tumor development by transgenic expression of a constitutively active insulin-like growth factor I receptor. Cancer Res 65: 3781–3787
22. Simpson KJ, Dugan AS, Mercurio AM 2004 Functional analysis of the contribution of RhoA and RhoC GTPases to invasive breast carcinoma. Cancer Res 64: 8694–8701
23. Pille JY, Denoyelle C, Varet J, Bertrand JR, Soria J, Opolon P, Lu H, Pritchard LL, Vannier JP, Malvy C, Soria C, Li H 2005 Anti-RhoA and anti-RhoC siRNAs inhibit the proliferation and invasiveness of MDA-MB-231 breast cancer cells in vitro and in vivo. Mol Ther 11:267–274
24. Wiseman BS, Werb Z 2002 Stromal effects on mammary gland development and breast cancer. Science 296: 1046–1049
25. Daniel CW, Silberstein GB, Strickland P 1987 Direct action of 17 β-estradiol on mouse mammary ducts analyzed by sustained release implants and steroid autoradiography. Cancer Res 47:6052–6057
26. Deugnier MA, Teuliere J, Faraldo MM, Thiery JP, Glukhova MA 2002 The importance of being a myoepithelial cell. Breast Cancer Res 4:224–230
27. Sternlicht MD, Kedeshian P, Shao ZM, Safarians S, Barsky SH 1997 The human myoepithelial cell is a natural tumor suppressor. Clin Cancer Res 3:1949–1958
28. Nguyen M, Lee MC, Wang JL, Tomlinson JS, Shao ZM, Alpaugh ML, Barsky SH 2000 The human myoepithelial cell displays a multifaceted anti-angiogenic phenotype. Oncogene 19:3449–3459
29. Barsky SH 2003 Myoepithelial mRNA expression profiling reveals a common tumor-suppressor phenotype. Exp Mol Pathol 74:113–122
30. Welm B, Freeman K, Chen M, Contreras A, Spencer D, Rosen J 2002 Inducible dimerization of FGFR1: development of a mouse model to analyze progressive transformation of the mammary gland. J Cell Biol 157:703–714
31. Wozniak MA, Desai R, Solski PA, Der CJ, Keely PJ 2003 ROCK-generated contractility regulates breast epithelial cell differentiation in response to the physical properties of a three-dimensional collagen matrix. J Cell Biol 163: 583–595
32. Settleman J 2001 Rac 'n Rho: the music that shapes a developing embryo. Dev Cell 1:321–331
33. Stanley ER, Berg KL, Einstein DB, Lee PS, Yeung YG 1994 The biology and action of colony stimulating factor-1. Stem Cells 12(Suppl 1):15–24; discussion 25
34. Lin EY, Gouon-Evans V, Nguyen AV, Pollard JW 2002 The macrophage growth factor CSF-1 in mammary gland

development and tumor progression. J Mammary Gland Biol Neoplasia 7:147–162
35. Sordella R, Jiang W, Chen GC, Curto M, Settleman J 2003 Modulation of Rho GTPase signaling regulates a switch between adipogenesis and myogenesis. Cell 113: 147–158
36. Deome KB, Faulkin Jr LJ, Bern HA, Blair PB 1959 Development of mammary tumors from hyperplastic alveolar nodules transplanted into gland-free mammary fat pads of female C3H mice. Cancer Res 19: 515–520
37. Rijnkels M, Rosen JM 2001 Adenovirus-Cre-mediated recombination in mammary epithelial early progenitor cells. J Cell Sci 114:3147–3153
38. Church GM, Gilbert W 1984 Genomic sequencing. Proc Natl Acad Sci USA 81:1991–1995

Molecular Endocrinology **is published monthly by The Endocrine Society (http://www.endo-society.org), the foremost professional society serving the endocrine community.**

Elsevier Editorial System(tm) for Developmental Biology

Manuscript Draft

Manuscript Number:

Title: Crosstalk between the p190-B RhoGAP and IGF signaling pathways is required for embryonic mammary bud development.

Article Type: Regular Article

Section/Category: Developmental Biology - Main

Keywords: ARHGAP5; IGF-1R; IRS-1; IRS-2; p63; androgen receptor; mammary gland; embryonic bud; epithelial-mesenchymal

Corresponding Author: Dr. Jeffrey M. Rosen,

Corresponding Author's Institution: Baylor College of Medicine

First Author: Brandy M Heckman

Order of Authors: Brandy M Heckman; Geetika Chakravarty, Ph.D.; Tracy Vargo-Gogola, Ph.D.; Maria Gonzales-Rimbau; Darryl L Hadsell, Ph.D.; Adrian V Lee, Ph.D.; Jeffrey Settleman, Ph.D.; Jeffrey M. Rosen

Manuscript Region of Origin:

Abstract: p190-B RhoGAP (p190-B, also known as ARHGAP5) has been shown previously to play an essential role in ductal morphogenesis in the postnatal mammary gland. Expression of p190-B is detected at E12.5 in the epithelium of the mammary anlage. Here we report that embryos with a homozygous p190-B gene deletion exhibit major defects in embryonic mammary bud development including smaller bud size, fewer p63-positive cells, and display characteristics of impaired mesenchymal proliferation. IGF-1R null embryos also contain similar small mammary buds and a loss of p63-staining cells. However, unlike the p190-B null embryos, the IGF-1R- homozygous embryos did not display similar mesenchymal defects. Since p190-B and IGF signaling intersect at the level of the IRS proteins, we examined IRS1/2 double knock-out embryonic mammary buds. We found that IRS1/2 double knock-out embryos exhibit major defects similar to those observed in the p190-B null embryos. Importantly, like the p190-B deficient buds, the proliferation of the IRS1/2 null mesenchyme is impaired. These results indicate that p190-B and IRS proteins acting possibly through IGF-1R and integrin signaling are critical for the migration of epithelial progenitors as well as the ensuing epithelial-mesenchymal interactions necessary to sustain mammary bud development and morphogenesis.

May 15, 2006

Robb Krumlauf
Stowers Institute for Medical Research
1000 E. 50th Street
Kansas City, MO 64110
Tel: +1 816 926 4051
Fax: +1 816 926 2008

Dear Robb:

Enclosed please find a copy of our manuscript entitled, "Crosstalk between p190-B RhoGAP and IGF signaling pathways in required for embryonic mammary bud development " by Brandy Heckman, Geetika Chakravarty, Tracy Vargo-Gogola, Maria Gonzales-Rimbau, Darryl Hadsell, Adrian Lee, Jeffrey Settleman and Jeffrey M. Rosen which we are submitting for consideration of publication in Developmental Biology. Our collaborator, Jeff Settleman's laboratory has previously reported in Developmental Cell the characterization of p190-B RhoGAP-null mice and the interactions of p190-B and Rho kinase with the IGF-I signal transduction pathway in p190-B-null MEFs. Previous studies from our laboratory have revealed that p190-B plays an essential role in mammary gland morphogenesis. These current results enhance a growing understanding of the molecular mechanisms that lead to embryonic mammary gland formation including establishing that p190-B and IRS-1/2 expression is essential for proper migration of mammary progenitor cells from the epidermis into the mammary bud as well as mesenchymal proliferation and differentiation.

Carmen Birchmeier would be an appropriate editor to handle this manuscript. As potential reviewers for this manuscript, we would like to suggest Dr. John Wysolmerski at yale, john.wysolmerski@yale.edu, Dr. Gertraude Robinson at the NIH, mammary@nih.gov, or Dr. Beatrice Howard at Institute of Cancer Research, London, England, beatrice.howard@icr.ac.uk, all of whom are experts on embryonic mammary gland development.

Thank you for your prompt handling of our manuscript.

Best wishes,

Jeffrey Rosen, Ph.D.,
C.C. Bell Professor of Molecular and Cellular Biology and Medicine

Suggested reviewers all of whom are experts on embryonic mammary gland development:

Dr. John Wysolmerski at Yale, john.wysolmerski@yale.edu

Dr. Gertraude Robinson at the NIH, mammary@nih.gov

Dr. Beatrice Howard at Institute of Cancer Research, London, England, beatrice.howard@icr.ac.uk,

Crosstalk between the p190-B RhoGAP and IGF signaling pathways is required for embryonic mammary bud development.

Heckman BM[1*], Chakravarty G[2*], Vargo-Gogola T[1], Gonzales-Rimbau M[1], Hadsell DL[3], Lee AV[4], Settleman J[5] and Rosen JM[1].

[1]Department of Molecular and Cellular Biology, Baylor College of Medicine, Houston, Texas 77030.[2]Department of Molecular & Cellular Oncology, MD Anderson Cancer Center, Houston, TX 77030.
[3]U.S. Department of Agriculture/Agricultural Research Service Children's Nutrition Research Center, Department of Pediatrics, Baylor College of Medicine, Houston, Texas 77030, USA.
[4]The Breast Center, Department of Medicine, Baylor College of Medicine, Houston, TX 77030
[5]Massachusetts General Hospital Cancer Center and Harvard Medical School, 149 13th Street, Charlestown, MA 02129, USA.
* Authors contributed equally to this work.

Key words: ARHGAP5, IGF-1R, IRS-1, IRS-2, p63, androgen receptor, mammary gland, embryonic bud, epithelial-mesenchymal

Corresponding author

Jeffrey M Rosen
Department of Molecular and Cellular Biology,
Baylor College of Medicine,
Houston, Texas 77030.
jrosen@bcm.edu.

Abstract:

p190-B RhoGAP (p190-B, also known as ARHGAP5) has been shown previously to play an essential role in ductal morphogenesis in the postnatal mammary gland. Expression of p190-B is detected at E12.5 in the epithelium of the mammary anlage. Here we report that embryos with a homozygous p190-B gene deletion exhibit major defects in embryonic mammary bud development including smaller bud size, fewer p63-positive cells, and display characteristics of impaired mesenchymal proliferation. IGF-1R null embryos also contain similar small mammary buds and a loss of p63-staining cells. However, unlike the p190-B null embryos, the IGF-1R- homozygous embryos did not display similar mesenchymal defects. Since p190-B and IGF signaling intersect at the level of the IRS proteins, we examined IRS1/2 double knock-out embryonic mammary buds. We found that IRS1/2 double knock-out embryos exhibit major defects similar to those observed in the p190-B null embryos. Importantly, like the p190-B deficient buds, the proliferation of the IRS1/2 null mesenchyme is impaired. These results indicate that p190-B and IRS proteins acting possibly through IGF-1R and integrin signaling are critical for the migration of epithelial progenitors as well as the ensuing epithelial-mesenchymal interactions necessary to sustain mammary bud development and morphogenesis.

Introduction

Mouse mammary gland development can first be detected as a line of epithelial cells that thicken between the limb buds at embryonic day 10.5-11.5 (E10.5-11.5) (Chu et al., 2004; DasGupta and Fuchs, 1999; Eblaghie et al., 2004; Veltmaat et al., 2004). The line fragments into individual placodes that appear as elevated domes, which then invaginate into the underlying dermal mesenchyme to form bulb-shaped buds at E12.5 (Mailleux et al., 2002). At E13 the bud enters a resting phase, and the mesenchyme of fibroblasts adjacent to the bud condenses into concentric rings that are separated from the bud by basement membrane (Kimata et al., 1985; Kratochwil, 1969). This process coincides with the increased expression of fibronectin, tenascin-C and androgen receptor, which distinguishes the mammary mesenchyme from the surrounding dermis and the underlying mesenchyme (Chiquet-Ehrismann et al., 1986; Durnberger and Kratochwil, 1980; Inaguma et al., 1988). The cells underlying the mammary mesenchyme condense to form the fat pad precursor at E14 (Sakakura et al., 1982). The fad pad precursor becomes less compact at E15-16 forming a loose connective tissue and producing fatty substances (Sakakura, 1991). During this time the bud undergoes rapid proliferation leading to bud elongation. The distal end of the primary sprout breaks through the mammary mesenchyme and penetrates the fat pad precursor. The mammary mesenchyme has been shown to be both permissive and instructive in mammary morphogenesis through a series of explant and tissue recombination experiments (Sakakura et al., 1976; Veltmaat et al., 2003).

Previous studies have demonstrated that p190-B interacts with the insulin-like growth factor (IGF) signaling pathway. In fibroblasts from p190-B null embryos, increased Rho kinase activity decreased IGF/insulin signaling to downstream pathways

components, leading to a reduction in phosphorylated p38, JNK, and Akt (Sordella et al., 2002). The IGF-1 receptor (IGF-1R) functions through activation of an intrinsic tyrosine kinase in its cytoplasmic domain (Sachev, 2001). Upon activation, the receptor becomes autophosphorylated and recruits intracellular substrates, including insulin receptor substrate (IRS) proteins. The IRS proteins (IRS-1,-2, -3, and -40, are adaptor molecules that organize signaling complexes at sites of receptor activation (White, 2002). IRS-1 and -2 are ubiquitously expressed including in mammary epithelium. IRS-3 and -4 are restricted in their localization, and are predominantly found in adipose tissue and brain, respectively (Lavan et al., 1997a; Lavan et al., 1997b; Lee et al., 2003).

Previous studies from our laboratory have demonstrated that p190-B interacts with the IGF-1R signaling pathway to regulate mammary ductal morphogenesis in virgin female mice (Chakravarty et al., 2003). Specifically, both deletion of IGF-1R or haploinsufficiency of p190-B resulted in decreased proliferation in the terminal end buds (TEBs) and delayed ductal elongation. Additionally, embryonic mammary transplantation studies from p190-B and IGF-1R null mice have shown that these pathways are essential for postnatal mammary gland development, since p190-B null transplants failed to grow out (Chakravarty et al., 2003), or exhibited only limited outgrowth potential in the case of IGF-1R (Bonnette and Hadsell, 2001). Loss of IRS-1 has been shown to reduce mammary fat pad size but is not critical for normal ductal development or pregnancy-induced proliferation although it was hypothesized that IRS-2 may compensate for the loss of IRS-1 expression (Lee et al., 2003). These data led us to further investigate the role of the p190-B and the IGF signaling pathways during embryonic mammary morphogenesis.

The studies presented here demonstrate an essential role for p190-B in the IGFR/IRS-1,2 signal transduction pathway during embryonic mammary morphogenesis. The data suggest that these pathways are critical for migration of epithelial progenitors. Furthermore, loss of either p190-B or IRS-1/2 results in major mesenchymal defects implicating this signaling network in the establishment of the epithelial-mesenchymal interactions that are necessary to sustain mammary bud development. These embryonic mammary defects help explain the previously observed failed postnatal ductal development of the p190-B-deficient mammary glands, which were dependent on alterations of the IGF signaling pathway.

Materials and Methods

Tissue preparation

Heterozygous females (p190-B C57Bl/6; IGF-RI FVB; IRS-1/IRS-2 FVB) were mated with heterozygous males with detection of a plug marked as E1. Pregnant females at E14.5 of pregnancy were injected with BrdU (100 mg/kg) intraperitoneally. Three hours later, embryos were dissected by Cesarean section in PBS and fixed overnight in 4% paraformaldehyde (PFA). Specimens were dehydrated and embedded in paraffin. Serial sections were then taken in the frontal plane at 7μm on probe on plus slides (Fisher Scientific). Prior to hybridization, the slides were deparaffinized in xylene, rehydrated, and fixed in 4% PFA for 30 min.

In situ hybridization

Riboprobes were labeled with [DIG]-UTP (Boehringer 1277073), using T7 transcription system from Stratagene. To generate antisense riboprobe template, p190B cDNA was

amplified from mouse brain by PCR using forward primer 5'-GGATCCTAATACGACTCACTATAGGGAGAATGAGATTTATGTTGTCCCAG and reverse primer 5'- GTAATTACTTTCCCAATTTCT. Sense riboprobe template was generated from the same cDNA by PCR using forward primer 5'-ATGAGATTTATGTTGTCCCAG and reverse primer 5'-GGATCCTAATACGACTCACTATAGGGAGAGTAATTACTTTCCCAATTTCT.

For whole mount in situs: Embryos were dissected and fixed in 4% PFA overnight, washed with 70% alcohol. To reduce the background, the embryos were bleached with 4:1 mix of ethanol and 30% H_20_2 for 1hr and treated with 15µg/ml proteinase K (PK) for 15 min. Proteinase K treatment was blocked with a short rinse in PBT followed by two washes in freshly prepared 2mg/ml glycine in PBT. Embryos were re-fixed with freshly prepared 0.2% glutaraldehyde/4%PFA/PBS for 20 min. Fixative was replaced with pre-warmed (68ºC) hybridization buffer (DAKO S3304) and rocked gently until the embryos sank (indicating that the formamide had penetrated the embryos). This hybridization buffer was replaced with fresh pre-warmed hybridization buffer containing the probe at a concentration of 1µg/ml and hybridized overnight at 68ºC. The embryos were then washed two times for 30 min each with freshly prepared pre-warmed solution I (50% Formamide, 5XSSC, 1%SDS) at 68ºC followed by another wash of 10 min in a prewarmed 1:1 mix of solutions I & solution II (0.5M NaCl, 10mM TrisHCl pH 7.5, 0.1% Tween 20) at 68ºC followed by 3 final washes of 5 min each with solution II at RT. Nonspecific hybridization was reduced by incubating the embryos for 30 min in 100ug/ml RNAase A in solution II at 37ºC. Excess RNAse A was removed with two 30 min washes with freshly prepared, prewarmed solution III (50% deionized formamide,

2XSSC) at 65ºC. Embryos were equilibrated with TBST containing 2mM levamisole and blocked with 10% FCS/2% blocking reagent (Roche, Mannheim,Germany 1096176)/2mM levamisole in TBST for at least 1 hr**.** This was followed by overnight incubation of the blocked embryos at 4ºC with 1:1000 anti-digoxigenin-AP antibody (Roche 1093274) supernatant solution diluted 1:1 in 10% FCS/2% blocking reagent/TBST/2mM levamisole. Subsequently they were washed with 2mM levamisole/TBST solution for 5 – 6 hrs and left overnight in fresh levamisole/TBST at 4ºC. Color development was initiated by washing the embryos with freshly prepared NTMT (100mM Nacl, 100mM TrisHCl pH 9.5, 50mM MgCl2, 0.1% Tween 20) +2mM Levamisole twice for 20 min and incubating them in prewarmed BM purple (Roche, 1442074) from 30 min to overnight in the dark at room temperature (RT). The stained embryos were post fixed with freshly prepared 4%PFA.

For embryo sections: paraffin sections (5μm) of E14.5 embryos were deparaffinized, rehydrated and washed in PBS, then treated with PK (25μg/ml) for 1 hr. at 37ºC and fixed with 4% PFA for 30 min followed by washing with 2xSSC. Pre-warmed hybridization buffer containing the probe at a concentration of 1μg/ml was added and hybridized overnight at 55ºC. Slides were washed with stringency buffer (50% 2xSSC, 50% Formamide) for 15 min at 42 ºC followed by washes with 2xSSC 20 min at RT and digestion with 40μg/ml of RNase A for 15 min at 37 ºC then washed with 0.1xSSC for15 min at 42 ºC and then 10 min at RT. Slides were then washed with Buffer I (100mM Tris pH 7.5, 150mM NaCl) for 5 min at RT and blocked for 2 hrs in Buffer I with 3% sheep serum and 0.3% triton X-100 at RT. The slides were then incubated overnight with 1:200 anti-digoxigenin-AP at 4 ºC. For color development slides were washed with Buffer I for

10 min at RT and then washed with Buffer II (100mM Tris pH 9.5, 100mM NaCl, 50mM MgCl) for 2 min at RT and incubating them in prewarmed BM purple (Roche Mannheim,Germany 1442074) from 30 min to overnight in the dark at RT. Slides were counterstained with nuclear fast red, dehydrated, and mounted using Permount (Sigma, St. Louis, MO).

Immunohistochemistry

Five to seven micrometer sections were incubated overnight at 37°C, deparaffinized with xylene, and rehydrated with ethanols. Heat-induced antigen retrieval was performed in 10mM citrate by boiling for 20 min. All washes were performed with PBS unless otherwise stated. Slides were then incubated with the respective antibodies p63 (Neomarkers, Fremont, CA MS-1081-P(Ab1): 1:500 in M.O.M diluent buffer (Vector Laboratories Burlingame, CA BMK-2202); androgen receptor (Upstate, Lake Placid, NY 06-680): 1:500 in 5% BSA, 0.5% blocking buffer; IRS-1 (Upstate, 06-248): 1:800 in 5% BSA, 0.5% blocking buffer; IRS-2 (Upstate, 06-506): 1:800 in 5% BSA, 0.5% blocking buffer; phospho-IRS(Ser612) (Biosource, Carlsbad, CA 44-816): 1:50 in 5% BSA, 0.5% blocking buffer; phospho-Akt(Ser473) (Cell Signaling, Danvers, MA 9277): 1:200 in 5% BSA, 0.5% blocking buffer; Biotin-conjugated BrdU (BD Pharmingen, San Jose, CA 550803): 1:10 in 5% BSA, 0.5% blocking buffer all incubated overnight at RT. Sections were washed in PBS and incubated with anti-rabbit (Oncogene Research, Darmstadt, Germany), or anti-mouse (Oncogene Research) secondary antibodies diluted 1:1000 in 5% BSA, 0.5% blocking buffer for 1 hr at RT. Vectastain Elite ABC and diaminobenzidine (DAB) substrate kits were used to detect immunoperoxidase staining according to the manufacturer's instructions (Vector Laboratories, Burlingame CA). As a

negative control, slides were incubated with purified rabbit immunoglobulin (The Jackson Laboratory, Bar Harbor, ME). Detection was achieved by incubation with diaminobenzidine (DAKO, Carpinteria, CA) for 10 min. Slides were counterstained with hematoxylin for 30 sec, dehydrated, and mounted using Permount.

Results

p190-B is expressed in the developing mammary anlagen

Previously it was reported that p190-B is ubiquitously expressed in most adult tissues. In contrast, p190-B is developmentally regulated throughout postnatal mammary gland development and function (Chakravarty et al., 2000). Lack of ductal outgrowths from p190-B null transplants indicated that its expression may also be spatiotemporally restricted during embryonic development. We examined this by performing whole mount *in situ* hybridization for p190-B expression on wildtype embryos. For this analysis, whole mount *in situs* were done on E8.5 embryos, prior to mammary development, and E12.5, a stage in mammary bud development where the spherical mammary placode differentiates into an epithelial bud. Although p190-B mRNA shares only 57% homology with p190-A at the nucleotide level, the specificity of p190-B antisense probe was further ascertained by aligning the probe sequence with that of mouse p190-A. In either case, no significant homology was detected between the two sequences.

Ubiquitous expression of p190-B was detectable as early as E8.5 (data not shown). By E12.5, strong expression was detected in the brain, spinal cord, skin, and the limbs (Figure 1a). At E12.5, the p190-B transcript is detected throughout the mammary epithelial bud compartment (Figure 1b). This was further confirmed by *in situ* hybridization in tissue sections at E14.5 where expression of p190-B is present in the epithelium and at a lower level in the surrounding mesenchyme in wildtype embryonic mammary buds (Figure 1c) as compared to the sense control (Figure 1d). This expression pattern and the lack of ductal outgrowth suggested p190-B might play an essential role in mammary placode formation and differentiation.

Loss of p190-B results in a smaller mammary bud size with a disorganized mesenchyme

While a number of signaling molecules have been shown to be expressed within the epithelium or mesenchyme of the developing bud, few have been shown to play a functional role. Since loss of p190-B resulted in complete failure of postnatal ductal development we examined whether p190-B deficiency also impacted formation and differentiation of the mammary anlagen. For this analysis, E14.5 embryos from all three genotypes were isolated and the histology of hematoxylin and eosin (H&E) stained sections was analyzed. Since the buds are known to form at different rates, a bud-to-bud comparison was done (Veltmaat et al., 2003). The wildtype buds (Figure 2a) had an organized epithelial center surrounded by a dense mesenchyme. The heterozygous buds displayed a variable intermediate phenotype. Some buds were comparable to the wildtype, while in others, the epithelium and surrounding mesenchyme appeared disorganized. In contrast, the buds from null embryos (n=3) exhibited markedly fewer epithelial cells and the mesenchyme surrounding the epithelium appeared to be diminished and disorganized (Figure 2c). Bud size was determined by quantifying the number of sections through which the bud can be seen, 3 buds each were counted from 3 independent animals. The graph shows that a significant decrease in bud size is observed in the heterozygous and null embryos as compared to the wildtype (Figure 2d).

To gain further insight into the role of p190-B signaling in placode formation, we examined the expression of markers of progenitor mammary epithelium and mesenchyme in tissues from the three genotypes. To evaluate possible alterations in progenitor epithelial content, the expression of p63 was compared in wildtype, heterozygous and

p190-B-deficient E14.5 mammary anlagen. p63 staining was seen in the epithelium of the mammary anlagen in wildtype mice (Figure 3a). Interestingly, a pronounced reduction in the number of p63-positive cells (n=3) was detected in the p190-B deficient embryos suggesting that fewer p63-positive epithelial progenitors had migrated into the bud (Figure 3c). As seen in Figure 3b, these changes were less dramatic in the heterozygous group of embryos.

To further evaluate the functional status of the mesenchyme, expression of Tenascin-C, a marker of mesenchymal differentiation, was examined in tissues from the three genotypes. In both the wildtype and heterozygous mice, Tenascin-C staining was clearly evident in the condensed mesenchyme (Figure 3d,e). However, mammary buds from the p190-B deficient mice consistently exhibited a reduction in the number of cells staining positive for Tenascin-C in the mesenchyme (n=3) (Figure 3f).

p190-B may interact with IGF-1R to cause migration of epithelial progenitors

Disruption of the gene for IGF-1R has also been shown to retard postnatal mammary development (Bonnette and Hadsell, 2001). In particular, it has been reported that IGF-1R null embryonic mammary buds display reduced growth potential when transplanted into syngeneic hosts. This phenotype is reminiscent of p190-B heterozygous transplants. However, it is less severe than the p190-B null transplants that completely failed to grow out, while the retarded IGF-1R transplants could be rescued by pregnancy (Bonnette and Hadsell, 2001). We, therefore, explored the possibility that loss of IGF-1R might also inhibit mammary anlagen formation and differentiation. To test this hypothesis, we analyzed mammary buds from IGF-1R -/- embryos both histologically

and through expression analysis of markers of epithelial and mesenchymal differentiation.

As shown in Figure 4, the H&E stained sagittal sections from E14.5 IGF-1R null embryonic mammary buds indicated that the smaller mammary bud phenotype of p190-B null mice was also mimicked in IGF-1R null mice. The wildtype buds had an organized epithelial center surrounded by a dense mesenchyme whereas the null buds displayed very little epithelium. However, unlike the p190-B null mice, these buds did not show any apparent mesenchymal defects. These observations were further confirmed by staining tissue sections from all three genotypes with both p63 and androgen receptor (AR) antibodies. The mammary buds from IGF-1R null mice had significantly reduced number of p63-positive cells (n=3) (Figure 4c-e), but did not appear to exhibit defects in AR staining (n=3) (Figure 4f-h). This result suggests that IGF-1R signaling is required for adequate migration of p63-positive progenitors into the mammary bud but loss of IGF-1R does not effect epithelial-mesenchymal interactions.

IRS-1/IRS-2 expression is decreased within the p190-B deficient mammary buds resulting in inhibition of downstream signaling

We previously reported that decreased expression of IRS-1 and -2 was observed in TEBs of p190-B heterozygous mice (Chakravarty et al., 2003). To examine if the downstream effectors of the IGF signaling pathway are affected in the p190-B null mammary buds, we examined the level of IRS-1 and IRS-2. The intensity of IRS-1 and IRS-2 staining was decreased within the epithelial compartment of the p190-B null (n=2) (Figure 5c,f) as compared to the wildtype mammary bud (Figure 5a,d). The level of IRS-1 and IRS-2 in the heterozygous bud (n=2) (Figure 5b,e) was intermediate between the

wildtype and IRS-1/2 null buds. Interestingly the IRS-1 expression is also decreased in the mesenchyme. These results suggest that lack of p190-B causes a decrease in IRS proteins, which may result in a loss of down stream signaling.

Fibroblasts from p190-B null embryos exhibited an increase in Rho kinase activity, which resulted in inhibition of IGF/insulin signaling as well as the activity of several downstream effectors including p38, JNK, and Akt (Sordella et al., 2002). This modulation of IGF signaling was shown to be due to phosphorylation of IRS-1 on Ser612 (Sordella et al., 2002). To examine a possible mechanism by which p190-B loss leads to a decrease in IRS-1 and if this affects downstream signaling, we examined the phosphorylation status of IRS-1 (Ser612) and active phospho-Akt (Ser473). Phospho-IRS-1 (Ser612) was increased in the p190-B null (Figure 5i) as compared to the wildtype (Figure 5g) and heterozygous (Figure 5h) mammary epithelial buds. Intense phospho-Akt staining was detected in the p190-B wildtype buds (Figure 5j), which was reduced to an intermediate level in the p190-B heterozygous mammary buds (Figure 4k) and further decreased in the p190-B null buds (Figure 5l). These results suggest that increased phosphorylation of IRS-1 may lead to loss of downstream signaling through Akt.

Loss of IRS-1/2 phenocopies loss of p190-B and reduces migration of epithelial progenitors and condensation of mammary mesenchyme

Since p190-B has been shown to regulate the level of IRS proteins both during ductal development and within the mammary bud, we hypothesized that loss of IRS-1 and IRS-2 may phenocopy the loss of p190-B (Chakravarty et al., 2003). To test this hypothesis, we analyzed mammary buds from IRS-1/2 double null embryos both

histologically and through expression analysis of markers of epithelial and mesenchymal differentiation.

As shown in Figure 6, the E14.5 IRS-1/2 double null embryos mimicked the smaller mammary bud phenotype seen in the IGF-1R null mice and the p190-B null mice. The wildtype buds (Figure 6a) displayed an organized epithelial center surrounded by a dense mesenchyme, whereas the double null buds displayed very little epithelium (Figure 6c). This was quantitated in the same manner as the p190-B null buds with 3 individual buds examined within 3 animals. A similar decease in size was seen in the IRS-1/2 heterozygote and null mammary buds (Figure 6d). However, unlike the IGF-1R null mice, the mesenchyme surrounding the epithelium appeared to be diminished and disorganized much like the p190-B null embryo. These observations were further confirmed by staining tissue sections of all three genotypes with both p63 and AR antibodies. The mammary buds from IRS-1/2 double null mice had significantly reduced staining for p63 (n=3) (Figure 7c), as well as a marked reduction in the number of cells staining positive for AR in the mesenchyme (n=3) (Figure 7f). Taken together, these results demonstrate that the IRS-1/2 null mammary buds phenocopy the p190-B deficient buds.

Loss of either p190-B or IRS1/2 leads to a defect in mesenchymal proliferation at E14.5

It is possible that p190-B affects the mesenchyme by either interrupting pathways necessary for differentiation or by modulating signaling pathways necessary for the proliferation of the mesenchyme. To investigate whether p190-B is required for mesenchymal proliferation, we examined cell proliferation by quantitating the number of

BrdU-positive cells associated with the mammary bud at day E14.5 (Figure 8a-c). As shown in Figure 8d, loss of p190-B resulted in a decrease in proliferation of the mesenchymal cells surrounding the E14.5 mammary bud ($p<.01$). This decrease was calculated by determining the percentage of BrdU-positive cells that also stained positive for AR in a serial section. As expected at this developmental stage, only a few of the epithelial cells within the E14.5 bud were proliferating, and no difference was observed in the epithelial proliferation between wildtype and p190-B null mammary buds as calculated by determining the percentage of BrdU-positive cells within the mammary epithelium. The IRS-1/2 null E14.5 mammary buds exhibited a similar decrease in the level of mesenchymal proliferation ($p<.01$) (Figure 8e). A significant decrease was also detected in the heterozygous IRS-1/2 mammary buds ($p<.03$). Importantly, there was no change in cleaved-caspase 3-positive cells in either the p190-B or IRS-1/2 mammary buds (data not shown), indicating there was no change is percentage of apoptotic cells. Two buds from 3 animals were analyzed from each genotype. These results coupled with the altered expression of mesenchymal markers indicate that both p190-B and the IRS proteins play a critical role in regulating the mesenchymal compartment within the developing mammary anlagen.

Discussion

Our results establish that p190-B expression is essential for proper migration of mammary progenitor cells from the epidermis into the mammary bud as well as mesenchymal proliferation and differentiation. IGF-1R loss leads to a similar decrease in migration of mammary progenitors but no detectable change in the mammary

mesenchyme. However, loss of both IRS-1 and IRS-2 phenocopies the loss of p190-B. This may be due to both the decrease in IRS-1/2 and an increase in serine 612 phosphorylation of IRS-1 resulting in the loss of IGF-1R signaling and its downstream effectors within the p190-B null bud.

Previous genetic studies have implicated several signaling pathways in various stages of bud development, such as fgf/fgfr, Lef-1/Tcf, Tbx-3, PTHrP/PTHrPR, and Eda/Edar(Hennighausen and Robinson, 2001). In the embryonic mammary gland at E12.5, p190-B was expressed in the mammary epithelium. By E14.5, the bud recruits condensed layers of mesenchyme that also express p190-B. In transplant studies p190-B heterozygous and IGF-1R null buds display retarded growth. However, while the p190-B null buds were incapable of any ductal outgrowth, the retarded IGF-RI null transplants could be rescued by pregnancy (Bonnette and Hadsell, 2001; Chakravarty et al., 2003). We, therefore, undertook a study to further characterize the role of this pathway in embryonic mammary gland development.

We postulated that the interaction of p190-B with the IGF-1R signaling pathway might affect the migration of epithelial progenitors that give rise to a differentiated mammary placode. Accordingly, we assessed the progenitor population in both models using the epithelial progenitor marker p63. P63 is a member of the p53 gene family that has been demonstrated to be critical for the regulation of proliferation and differentiation in epithelial progenitor cells (Koster et al., 2004; Mills et al., 1999). In normal adult breast tissue, p63 immunoreactivity is confined to the nuclei of myoepithelial cells and forms a continuous basal rim along the epithelial structures (Barbareschi et al., 2001). However, it is likely that there is a switch in p63 isoforms during development, which

cannot be distinguished by the p63 antibodies currently available. Previous work in the skin suggests a dual role for p63 in initiating stratification and maintaining proliferative potential (Koster et al., 2004). However, Mills et.al.(Mills et al., 1999) and Yang et.al. (Yang et al., 1999) have reported that mice homozygous for a disrupted p63 gene lack embryonic mammary buds, as well as other epithelial derivatives such as the lacrymal and salivary glands, due to defective epithelial-mesenchymal signaling. In addition, germline mutations in the p63 gene have been associated with severe mammary developmental defects in both mice and humans (van Bokhoven et al., 2001). Since p190-B null mice possessed all five pairs of mammary buds (data not shown), it was likely that mammary bud development was impaired during migration of the epidermal epithelium into the mammary bud. Mammary buds from IGF-1R null mice had very few p63-positive cells, suggesting that both IGF-1R and p190-B were required for the migration of this population into the mammary bud. This observation is consistent with a decrease in migration seen in p190-B null MEFs (unpublished data, J. Settleman). The scaffolding protein for activated C kinase(RACK1) which has been shown to modulate IGF-1R and ß1-integrin interactions (Kiely et al., 2005) and regulates cell adhesion, has also been shown to interact with p190-B(unpublished data, J. Settleman), thus, providing another connection between p190-B, IGF-1R signaling and cell adhesion and migration.

However, the p190-B null phenotype is clearly more severe than the phenotype caused by loss of IGF-1R alone. To determine if proteins within the IGF signaling pathway were modulated by loss of p190-B we examined IRS-1, IRS-2, phospho-IRS-1(Ser612), and phospho-Akt (Ser473). Immunohistochemistry analysis demonstrated decreased expression of both IRS-1 and IRS-2 in the p190-B null mammary buds.

However, it appears that only IRS-1 is downregulated in the mesenchyme. This is consistent with previously published data from Sordella *et al.* (Sordella et al., 2002) that linked p190-B to IGF signaling via the modulation of Rho kinase and IRS-1 levels. There is also an increase in phospho-IRS-1, which was shown previously to lead to degradation, decreased IGF-1 signaling, and a decrease in transcription as a result of the loss of phospho-cAMP response element binding (CREB) protein. This decrease in IRS proteins has also been observed in the ductal development of p190-B heterozygous mice (Chakravarty et al., 2003). We also observed a decrease in phospho-Akt, a downstream target of IGF signaling.

The decrease in IRS proteins within the p190-B deficient mammary buds prompted us to examine mammary bud morphogenesis in IRS-1/2 double null E14.5 embryos. Lack of IRS-1 and IRS-2 fully recapitulated the phenotype including the mesenchymal defect observed in the p190-B null mammary anlage. IRS-1/2 null mammary buds also have a reduced number of p63-positive mammary progenitors. Interestingly, the phosphorylation of IRS proteins following integrin engagement has been reported to promote increased cell motility (Reiss et al., 2001; Shaw, 2001). Immunohistochemistry for AR marks the condensed mammary mesenchyme, which is reduced in the p190-B null and the IRS-1/2 double null but not the IGF-1R null mice. This lack of mesenchyme condensation was shown to be due to a decrease in mesenchymal proliferation with no increase in apoptosis detected as determined by cleaved-caspase 3 in both p190-B and IRS-1/2 null embryos. Previous studies have revealed that DNA synthesis in the stroma surrounding TEBs in the postnatal mammary gland is required for recruitment of migratory white blood cells, macrophages and

eosinophils, which are essential for normal end bud development (Silberstein, 2001). It is attractive to speculate that this decrease in mesenchyme due to the lack of proliferation may be responsible for the failure of transplanted p190-B null embryonic buds to grow out and form a mature ductal epithelium.

These current results enhance a growing understanding of the molecular mechanisms that lead to embryonic mammary gland formation. The roles of p190-B RhoGAP are diverse and include involvement in proliferation(Chakravarty et al., 2003; Su et al., 2003), cell transformation (Ellis et al., 1990), EMT(Ozdamar et al., 2005), integrin signaling(Burbelo et al., 1995), cytoskeletal reorganization(Hall, 1998), and development (Sordella et al., 2002). Many of these contrasting functions may be attributed to its large molecular weight, the presence of multiple protein motifs, its ability to act as a scaffold, and its capacity to interact with various chromatin remodeling complexes through its GAP domain (Nagaraja and Kandpal, 2004). Further studies including *in vivo* mammary bud specific gene arrays and pathway specific inhibitor studies will yield more insight into the roles of p190-B and IRS-1/2 in embryonic mammary bud development.

ACKNOWLEDGEMENTS

These studies were supported through NIH grant CA030195. T. V-G. is supported by a Department of Defense Breast Cancer Research Program fellowship DAMD17-1-03-0325. Thanks to Mr. Walter Olea for technical assistance with the IRS knockout mice and Kathryn Fewell and Remigo Lopez from the Breast Center Pathology Core for the phospho-IRS staining and embryo sectioning, respectively.

Figure Legend:

Figure 1: *p190-B is expressed throughout the differentiating mammary anlagen.* Whole-mount *in situ* hybridization of wildtype, E12.5 embryos with p190-B antisense riboprobe showing strong transcript expression in the in the developing mammary anlagen (a) low magnification, (b) high magnification. Spatial localization of *p190-B* mRNA in E14.5 mammary buds of *p190-B* +/+ mice using DIG-labeled antisense riboprobe. Shown are representative antisense (c) and sense (d) images with strong transcript expression in the epithelial compartment of the mammary bud and lower expression in the mesenchyme. Scale bar 50 μm (c,d).

Figure 2: *p190-B-/- mice possess distinct embryonic mammary buds but have reduced epithelial content and exhibit marked reduction of the mammary mesenchyme.* Sagittal sections of E14.5 embryonic mammary buds were stained with hematoxylin and eosin (H&E) to demonstrate a bud to bud comparison of the reduced number of epithelial cells and loss of a well-defined condensed mesenchyme around the p190-B-null (c) and heterozygous (b) buds compared to wildtype (a). Bud size is significantly decreased as shown by quantization of 3 buds from 3 animals of each genotype (d). Scale bar 50 μm.

Figure 3: *Loss of p190-B results in reduced epithelial content and a marked reduction in mammary mesenchyme.* p63 expression in the epithelium of E14.5 mammary buds of (a)p190-B wildtype, (b)p190-B heterozygous & (c)p190-B null mice. Tenescin-C is expressed in the condensed mesenchyme surrounding the epithelial buds in (d) wildtype

and (e)heterozygotes however, its expression is dramatically reduced in p190-B-null embryonic mammary buds (f). Scale bar 50 μm.

Figure 4: *IGF-1R null mice phenocopy the small mammary bud phenotype of p190-B$^{-/-}$ mice, but not the mesenchymal defect.* Shown here are the sagittal sections from wildtype and IGF-1R null E14.5 embryonic mammary buds stained with H&E. Note the smaller mammary buds in the nulls (b) as compared to the wildtype (a) littermates. p63 expression in the epithelium of E14.5 mammary buds of (c)IGF-1R$^{+/+}$, (d) IGF-1R $^{+/-}$ & (e) IGF-1R $^{-/-}$ mice. AR expression can be detected in the condensed mesenchyme of (f) wildtype, (g) heterozygotes and (h) IGF-1R null embryonic mammary buds. In panel (h) the mammary placode is not seen due to the plane of section used for staining. Scale bar 100 μm (a,b); 50 μm (c-h).

Figure 5: *Decreased IRS protein expression and phospho-Akt in p190-B null mammary buds* Sagittal sections of E14.5 embryonic mammary buds stained with IRS-1 (a-c); IRS-2 (d-f); phosphor-IRS-1(Ser612)(g-i); phosphor-Akt(Ser473)(j-l). Note the reduction in IRS-1, IRS-2, and phosphor-Akt in the p190-B null buds (c,f,l) as compared to the wildtype (a,d,j). An increase in phopho-IRS-1 is observed in the epithelium of p190-B null buds (i) as compared to wildtype (g). Scale bar 50 μm.

Figure 6: *Defective epithelial and mesenchymal differentiation in IRS1/2-deficient mice.* Sagittal sections of E14.5 embryonic mammary buds stained with H&E to demonstrate a bud to bud comparison of the reduced number of epithelial cells and loss of a well

defined condensed mesenchyme around the IRS1/2-null (c) and heterozygous (b) buds compared to wildtype (a). Bud size is significantly decreased as shown by quantization of 3 buds from 3 animals of each genotype (d). Scale bar 50 μm.

Figure 7: *Loss of IRS1/2 expression results in reduced bud size and disrupted mesenchyme at E14.5.* p63 expression in the epithelium of E14.5 mammary buds of (a)IRS1/2$^{+/+}$, (b) IRS1/2$^{+/-}$, (c) IRS1/2$^{-/-}$ mice. Note the dramatic reduction in the number of epithelial cells that stain for p63 both in the heterozygous (b) and IRS1/2-null mammary placodes (c). AR is expressed in the condensed mesenchyme surrounding the epithelial buds in (d) wildtype and (e) heterozygotes however; its expression is dramatically reduced in IRS1/2-null embryonic mammary buds (f). Scale bar 50 μm.

Figure 8: *Loss of either p190-B or IRS1/2 leads to a defect in mesenchymal proliferation at E14.5.* Saggital sections of E14.5 mammary buds stained for BrdU. Loss of p190-B (c) leads to a reduced number of BrdU-positive cells in the mesenchyme compared to wildtype (a) and heterozygous (b). BrdU/AR-double positive cells were counted as proliferating mesenchyme. Loss of p190-B (d) or IRS1/2 (e) leads to a decrease in the percentage of proliferating mesenchymal cellsas shown by quantization of 2 buds from 3 animals of each genotype. Scale bar 50 μm.

Barbareschi, M., Pecciarini, L., Cangi, M. G., Macri, E., Rizzo, A., Viale, G., and Doglioni, C. (2001). p63, a p53 homologue, is a selective nuclear marker of myoepithelial cells of the human breast. *Am J Surg Pathol 25(8):1054-60.*

Bonnette, S. G., and Hadsell, D. L. (2001). Targeted disruption of the IGF-I receptor gene decreases cellular proliferation in mammary terminal end buds. *Endocrinology Nov;142(11):4937-45.*

Burbelo, P. D., Miyamoto, S., Utani, A., Brill, S., Yamada, K. M., Hall, A., and Yamada, Y. (1995). p190-B, a new member of the Rho GAP family, and Rho are induced to cluster after integrin cross-linking. *J Biol Chem 1995* ***270****:30919-26.*

Chakravarty, G., Hadsell, D., Buitrago, W., Settleman, J., and Rosen, J. M. (2003). p190-B RhoGAP regulates mammary ductal morphogenesis. *Mol Endocrinol* **17,** 1054-65.

Chakravarty, G., Roy, D., Gonzales, M., Gay, J., Contreras, A., and Rosen, J. M. (2000). P190-B, a Rho-GTPase-activating protein, is differentially expressed in terminal end buds and breast cancer. *Cell Growth Differ 2000****11****:343-54.*

Chiquet-Ehrismann, R., Mackie, E. J., Pearson, C. A., and Sakakura, T. (1986). Tenascin: an extracellular matrix protein involved in tissue interactions during fetal development and oncogenesis. *Cell* **47,** 131-9.

Chu, E. Y., Hens, J., Andl, T., Kairo, A., Yamaguchi, T. P., Brisken, C., Glick, A., Wysolmerski, J. J., and Millar, S. E. (2004). Canonical WNT signaling promotes mammary placode development and is essential for initiation of mammary gland morphogenesis. *Development* **131,** 4819-29.

DasGupta, R., and Fuchs, E. (1999). Multiple roles for activated LEF/TCF transcription complexes during hair follicle development and differentiation. *Development* **126,** 4557-68.

Durnberger, H., and Kratochwil, K. (1980). Specificity of tissue interaction and origin of mesenchymal cells in the androgen response of the embryonic mammary gland. *Cell* **19,** 465-71.

Eblaghie, M. C., Song, S. J., Kim, J. Y., Akita, K., Tickle, C., and Jung, H. S. (2004). Interactions between FGF and Wnt signals and Tbx3 gene expression in mammary gland initiation in mouse embryos. *J Anat* **205,** 1-13.

Ellis, C., Moran, M., McCormick, F., and Pawson, T. (1990). Phosphorylation of GAP and GAP-associated proteins by transforming and mitogenic tyrosine kinases. *Nature* **343,** 377-81.

Hall, A. (1998). Rho GTPases and the actin cytoskeleton. *Science 1998* ***279****:509-14.*

Hennighausen, L., and Robinson, G. W. (2001). Signaling pathways in mammary gland development. *Dev Cell 2001* ***1****:467-75.*

Inaguma, Y., Kusakabe, M., Mackie, E. J., Pearson, C. A., Chiquet-Ehrismann, R., and Sakakura, T. (1988). Epithelial induction of stromal tenascin in the mouse mammary gland: from embryogenesis to carcinogenesis. *Dev Biol* **128,** 245-55.

Kiely, P. A., Leahy, M., O'Gorman, D., and O'Connor, R. (2005). RACK1-mediated integration of adhesion and insulin-like growth factor I (IGF-I) signaling and cell migration are defective in cells expressing an IGF-I receptor mutated at tyrosines 1250 and 1251. *J Biol Chem* **280,** 7624-33.

Kimata, K., Sakakura, T., Inaguma, Y., Kato, M., and Nishizuka, Y. (1985). Participation of two different mesenchymes in the developing mouse mammary gland: synthesis of basement membrane components by fat pad precursor cells. *J Embryol Exp Morphol* **89,** 243-57.

Koster, M. I., Kim, S., Mills, A. A., DeMayo, F. J., and Roop, D. R. (2004). p63 is the molecular switch for initiation of an epithelial stratification program. *Genes Dev* **18,** 126-31.

Kratochwil, K. (1969). Organ specificity in mesenchymal induction demonstrated in the embryonic development of the mammary gland of the mouse. *Developmental Biology* **20,** 46-71.

Lavan, B. E., Fantin, V. R., Chang, E. T., Lane, W. S., Keller, S. R., and Lienhard, G. E. (1997a). A novel 160-kDa phosphotyrosine protein in insulin-treated embryonic kidney cells is a new member of the insulin receptor substrate family. *J Biol Chem* **272,** 21403-7.

Lavan, B. E., Lane, W. S., and Lienhard, G. E. (1997b). The 60-kDa phosphotyrosine protein in insulin-treated adipocytes is a new member of the insulin receptor substrate family. *J Biol Chem* **272,** 11439-43.

Lee, A. V., Zhang, P., Ivanova, M., Bonnette, S., Oesterreich, S., Rosen, J. M., Grimm, S., Hovey, R. C., Vonderhaar, B. K., Kahn, C. R., Torres, D., George, J., Mohsin, S., Allred, D. C., and Hadsell, D. L. (2003). Developmental and hormonal signals dramatically alter the localization and abundance of insulin receptor substrate proteins in the mammary gland. *Endocrinology* **144,** 2683-94.

Mailleux, A. A., Spencer-Dene, B., Dillon, C., Ndiaye, D., Savona-Baron, C., Itoh, N., Kato, S., Dickson, C., Thiery, J. P., and Bellusci, S. (2002). Role of FGF10/FGFR2b signaling during mammary gland development in the mouse embryo. *Development* **129,** 53-60.

Mills, A. A., Zheng, B., Wang, X. J., Vogel, H., Roop, D. R., and Bradley, A. (1999). p63 is a p53 homologue required for limb and epidermal morphogenesis. *Nature 1999* ***398****:708-13.*

Nagaraja, G. M., and Kandpal, R. P. (2004). Chromosome 13q12 encoded Rho GTPase activating protein suppresses growth of breast carcinoma cells, and yeast two-hybrid screen shows its interaction with several proteins. *Biochem Biophys Res Commun* **313,** 654-65.

Ozdamar, B., Bose, R., Barrios-Rodiles, M., Wang, H. R., Zhang, Y., and Wrana, J. L. (2005). Regulation of the polarity protein Par6 by TGFbeta receptors controls epithelial cell plasticity. *Science* **307,** 1603-9.

Reiss, K., Wang, J. Y., Romano, G., Tu, X., Peruzzi, F., and Baserga, R. (2001). Mechanisms of regulation of cell adhesion and motility by insulin receptor substrate-1 in prostate cancer cells. *Oncogene* **20,** 490-500.

Sachev, D., and D. Yee. (2001). The IGF System and breast cancer. *Endocr Relat Cancer* **8,** 197-209.

Sakakura, T. (1991). New aspects of stroma-parenchyma relations in mammary gland differentiation. *Int Rev Cytol 125:165-202.*

Sakakura, T., Nishizuka, Y., and Dawe, C. J. (1976). Mesenchyme-dependent morphogenesis and epithelium-specific cytodifferentiation in mouse mammary gland. *Science Dec 24;194(4272):1439-41.*

Sakakura, T., Sakagami, Y., and Nishizuka, Y. (1982). Dual origin of mesenchymal tissues participating in mouse mammary gland embryogenesis. *Dev Biol* **91,** 202-7.

Shaw, L. M. (2001). Identification of insulin receptor substrate 1 (IRS-1) and IRS-2 as signaling intermediates in the alpha6beta4 integrin-dependent activation of phosphoinositide 3-OH kinase and promotion of invasion. *Mol Cell Biol* **21,** 5082-93.

Silberstein, G. B. (2001). Tumour-stromal interactions. Role of the stroma in mammary development. *Breast Cancer Res* **3,** 218-23.

Sordella, R., Classon, M., Hu, K. Q., Matheson, S. F., Brouns, M. R., Fine, B., Le, Z., Takami, H., Yamada, Y., and Settleman, J. (2002). Modulation of CREB Activity by the Rho GTPase Regulates Cell and Organism Size during Mouse Embryonic Development. *Dev Cell;2(5):553-65.*

Su, L., Agati, J. M., and Parsons, S. J. (2003). p190RhoGAP is cell cycle regulated and affects cytokinesis. *J Cell Biol* **163,** 571-82.

van Bokhoven, H., Hamel, B. C., Bamshad, M., Sangiorgi, E., Gurrieri, F., Duijf, P. H., Vanmolkot, K. R., van Beusekom, E., van Beersum, S. E., Celli, J., Merkx, G. F., Tenconi, R., Fryns, J. P., Verloes, A., Newbury-Ecob, R. A., Raas-Rotschild, A., Majewski, F., Beemer, F. A., Janecke, A., Chitayat, D., Crisponi, G., Kayserili, H., Yates, J. R., Neri, G., and Brunner, H. G. (2001). p63 Gene mutations in eec syndrome, limb-mammary syndrome, and isolated split hand-split foot malformation suggest a genotype-phenotype correlation. *Am J Hum Genet* **69,** 481-92.

Veltmaat, J. M., Mailleux, A. A., Thiery, J. P., and Bellusci, S. (2003). Mouse embryonic mammogenesis as a model for the molecular regulation of pattern formation. *Differentiation* **71,** 1-17.

Veltmaat, J. M., Van Veelen, W., Thiery, J. P., and Bellusci, S. (2004). Identification of the mammary line in mouse by Wnt10b expression. *Dev Dyn* **229,** 349-56.

White, M. F. (2002). IRS proteins and the common path to diabetes. *Am J Physiol Endocrinol Metab* **283,** E413-22.

Yang, A., Schweitzer, R., Sun, D., Kaghad, M., Walker, N., Bronson, R. T., Tabin, C., Sharpe, A., Caput, D., Crum, C., and McKeon, F. (1999). p63 is essential for regenerative proliferation in limb, craniofacial and epithelial development. *Nature 1999* ***398****:714-8.*

Figure 1

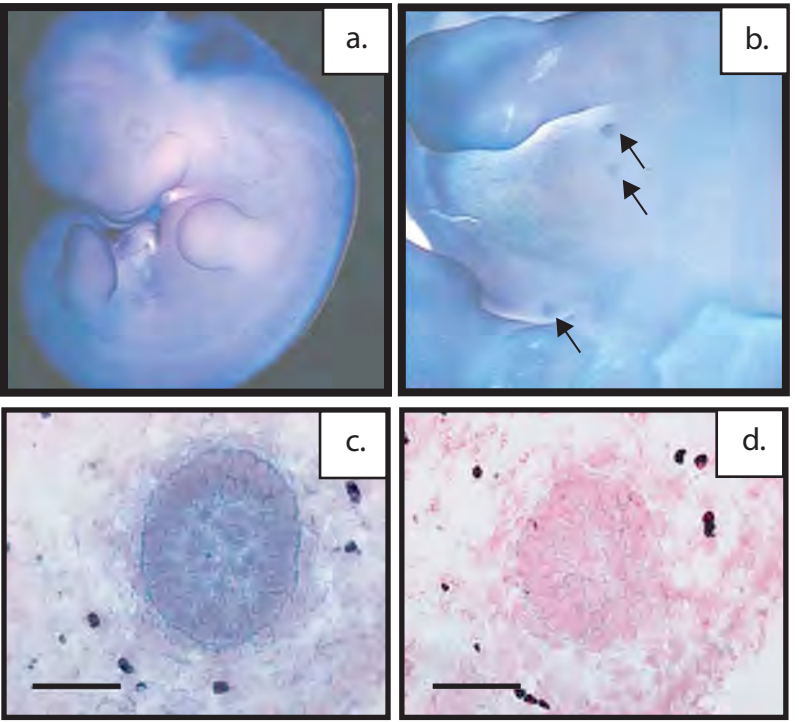

Figure 2

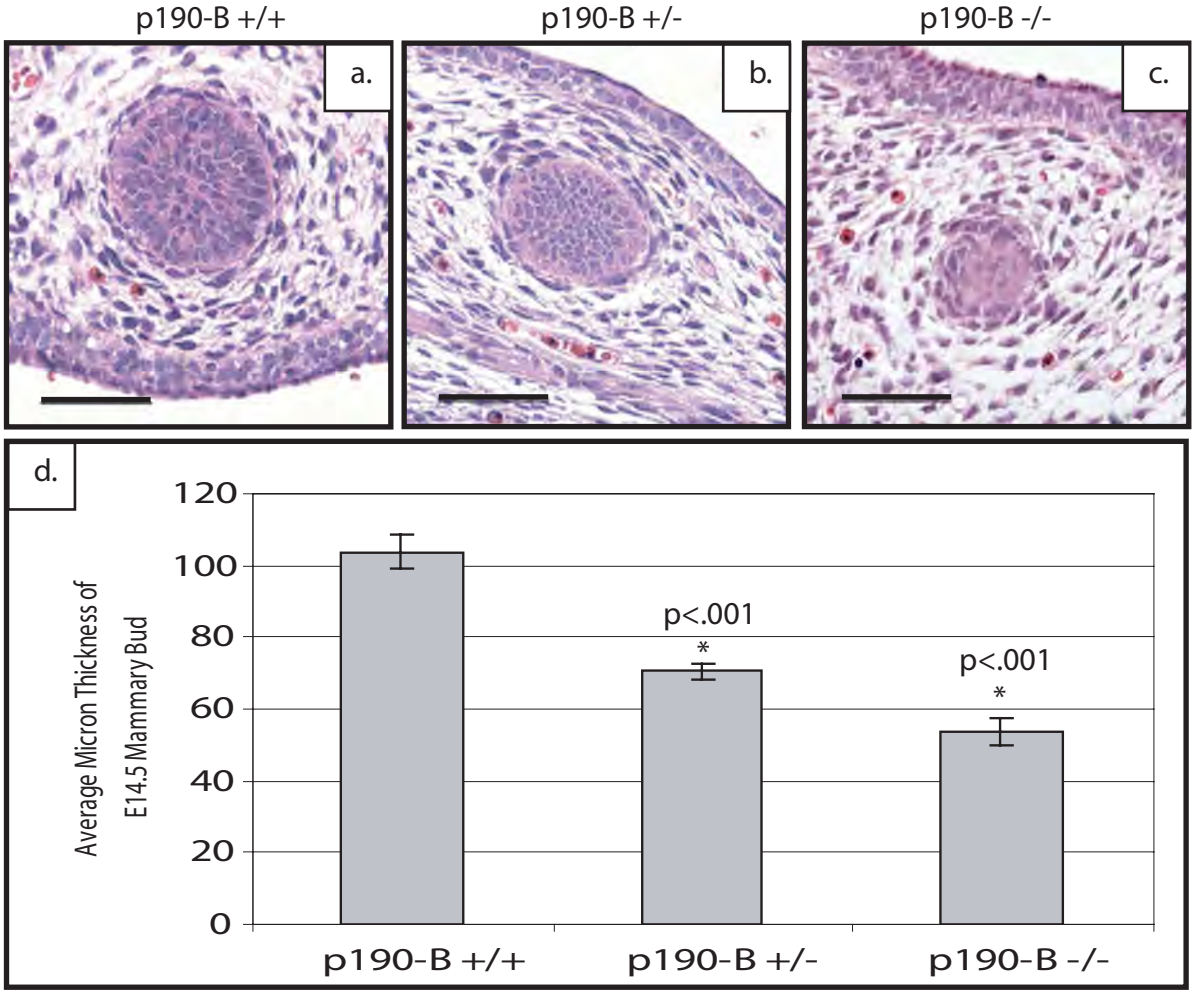
p190-B +/+
p190-B +/-
p190-B -/-
Bud 2
a.
b.
c.
d.
Average Micron Thickness of E14.5 Mammary Bud
120
100
80
60
40
20
0
p<.001
*
p<.001
*
p190-B +/+
p190-B +/-
p190-B -/-

Figure 3

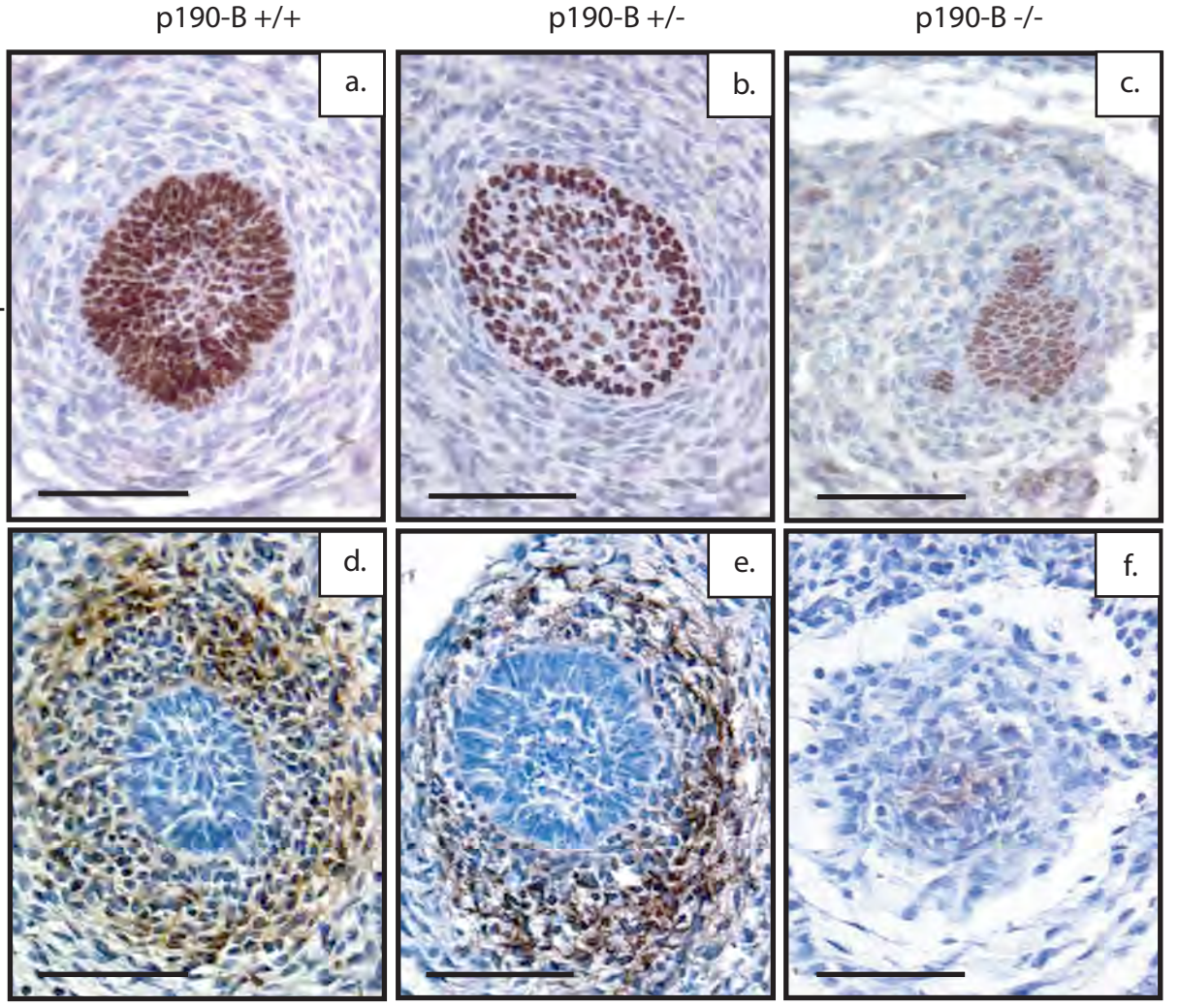

Figure 4

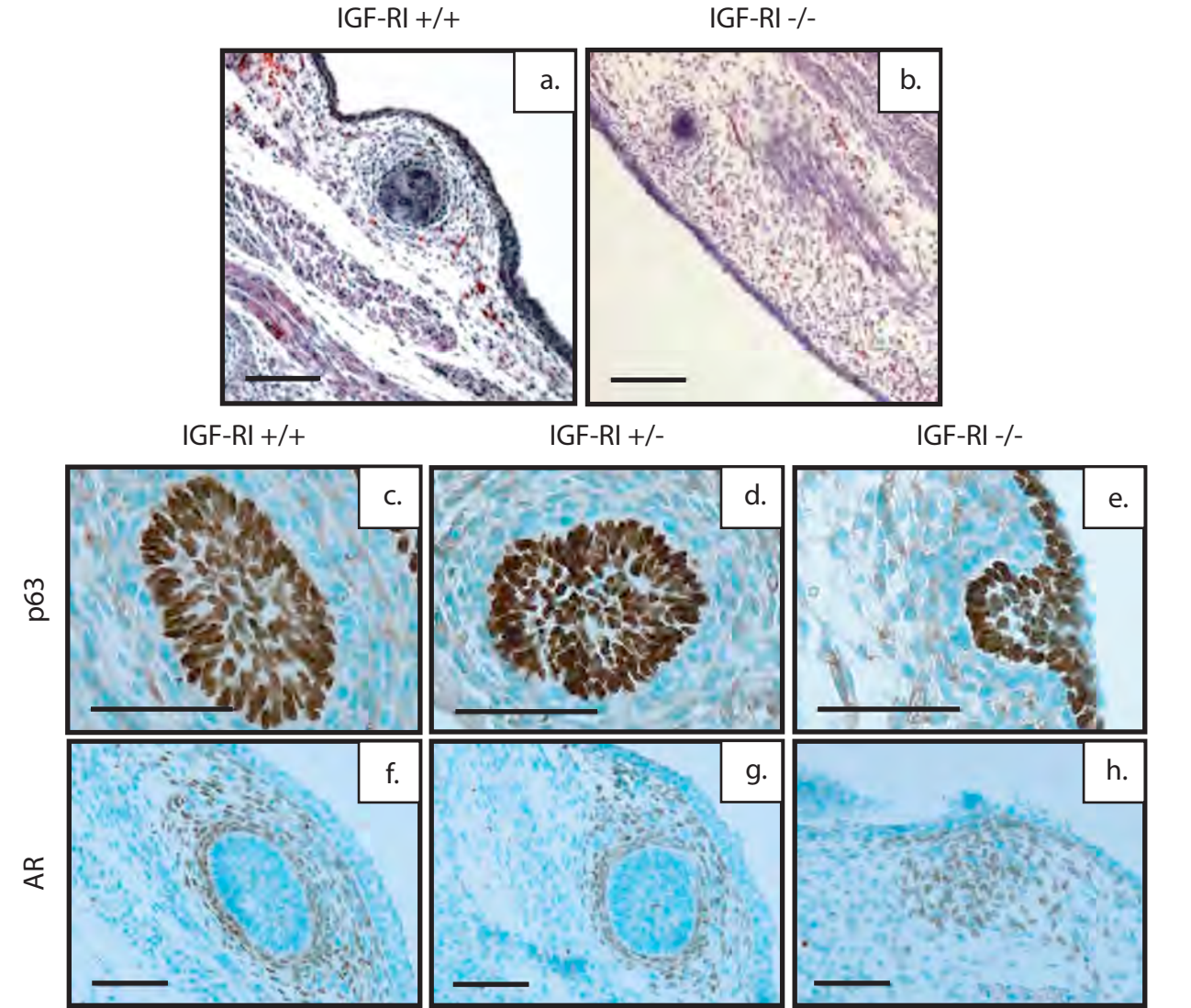

Figure 5

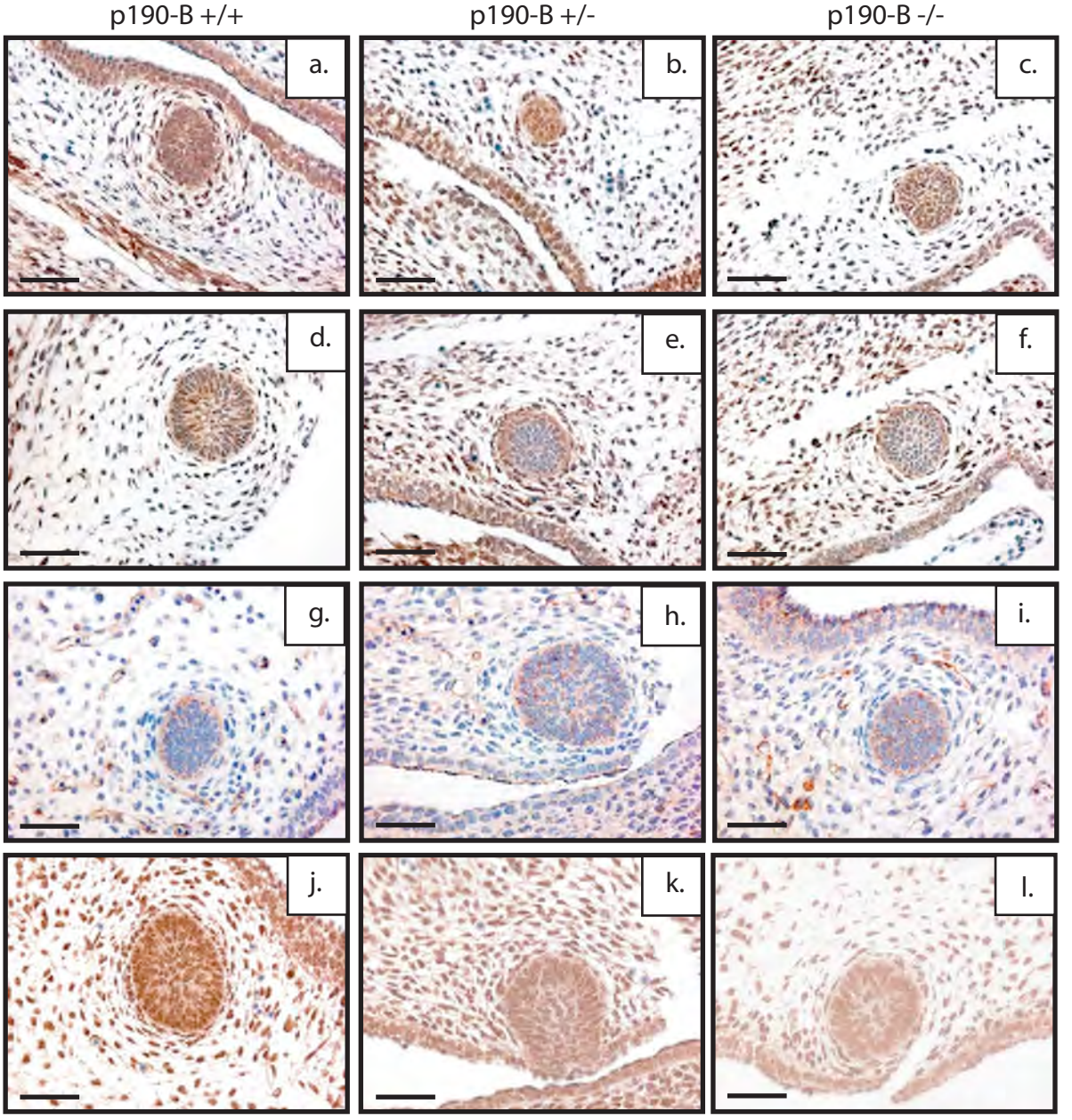

Figure 6

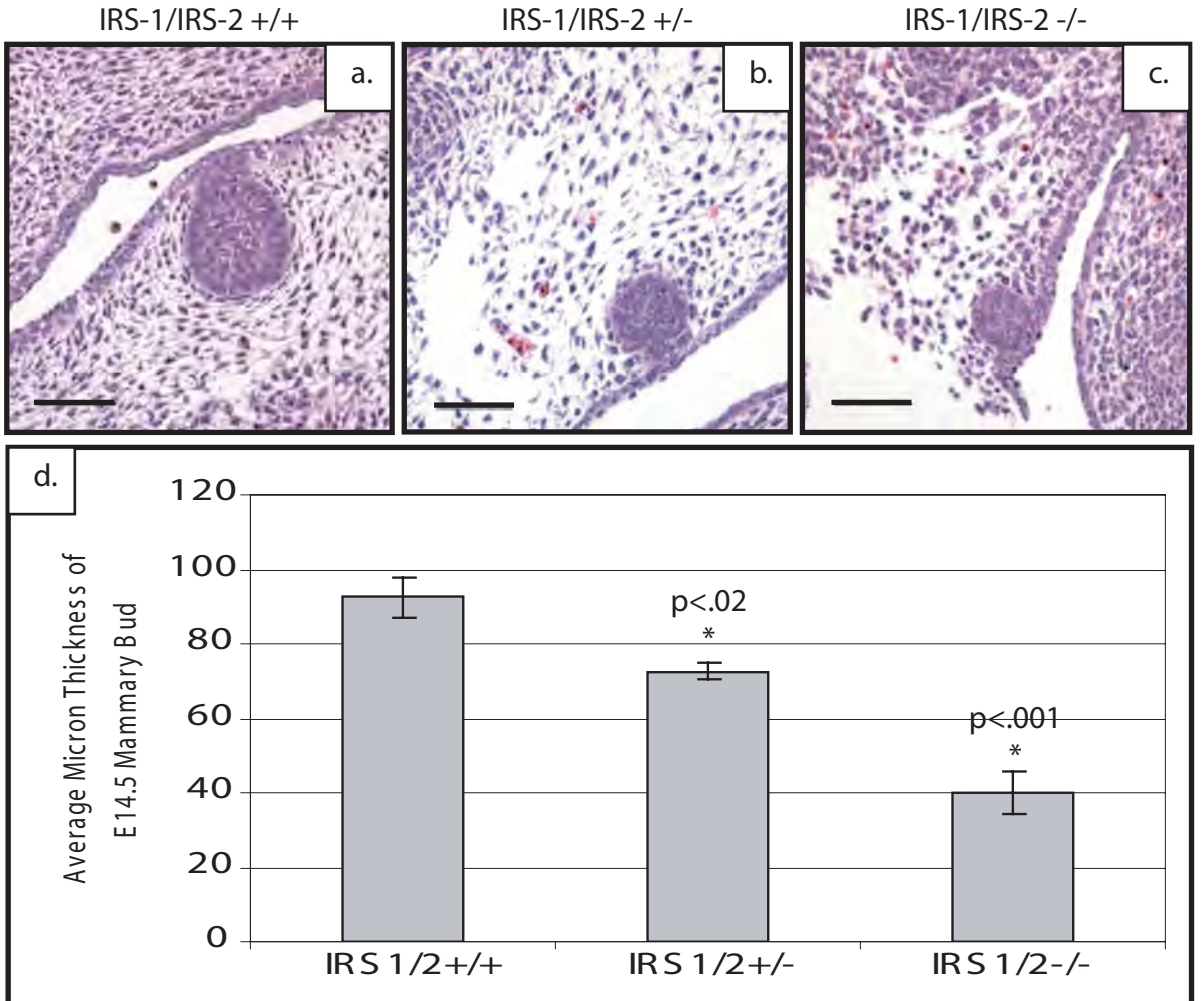
IRS-1/IRS-2 +/+
IRS-1/IRS-2 +/-
IRS-1/IRS-2 -/-
Bud 2
a.
b.
c.
d.
Average Micron Thickness of E14.5 Mammary Bud
120
100
80
60
40
20
0
p<.02
*
p<.001
*
IRS 1/2+/+
IRS 1/2+/-
IRS 1/2-/-

Figure 7

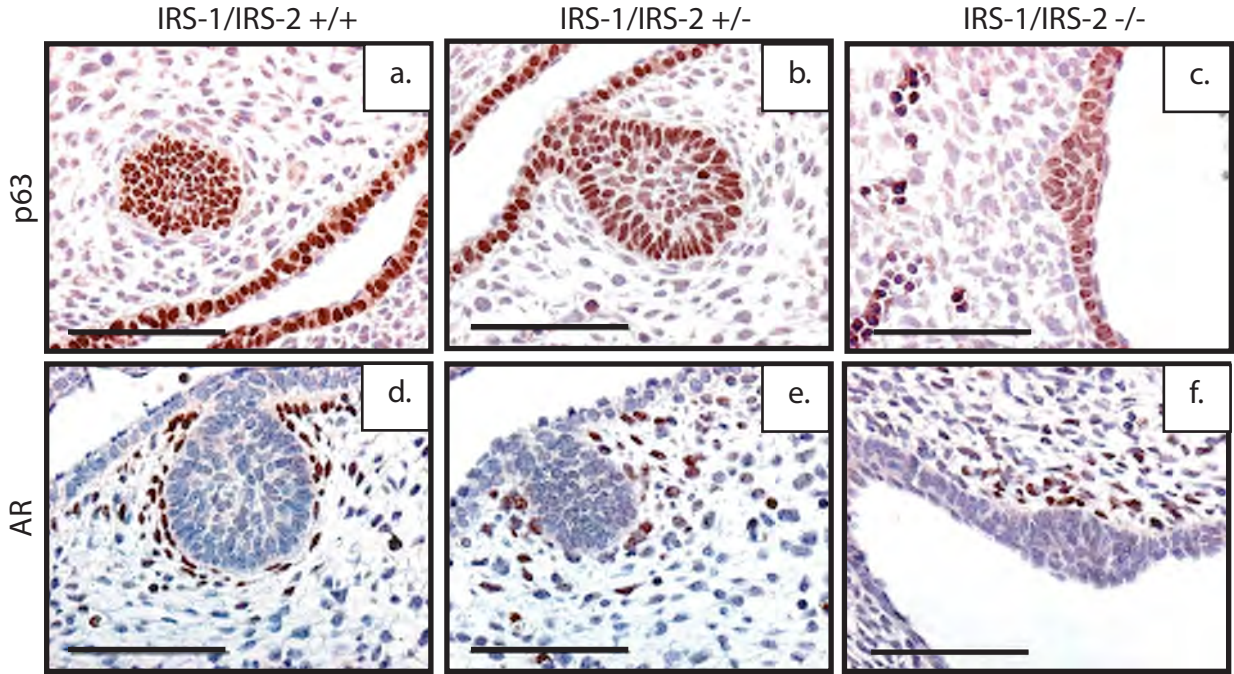

Figure 8

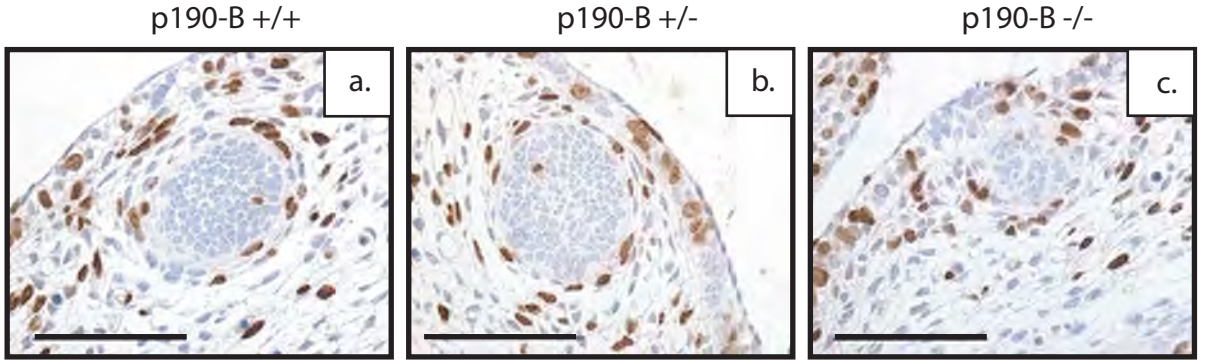
p190-B +/+
p190-B +/-
p190-B -/-
BrdU
a.
b.
c.

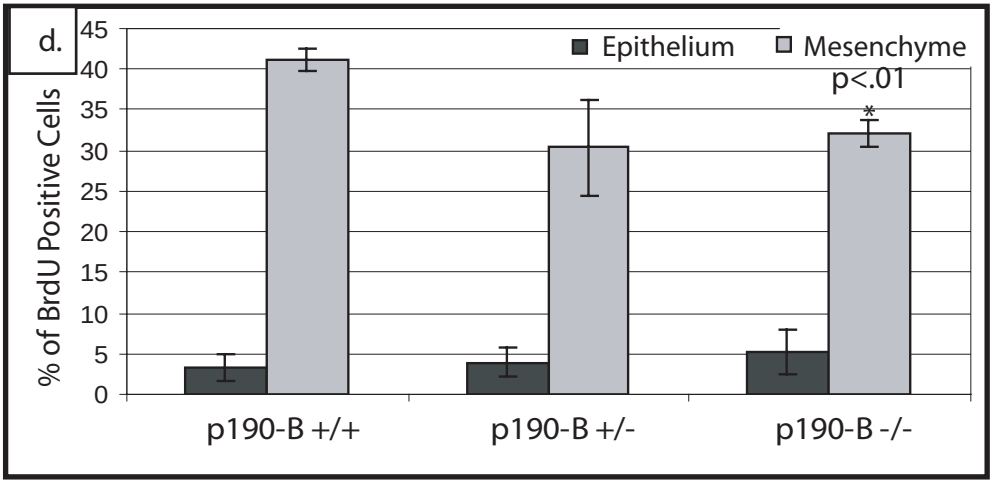
d.
Epithelium
Mesenchyme
% of BrdU Positive Cells
45
40
35
30
25
20
15
10
5
0
p<.01
*
p190-B +/+
p190-B +/-
p190-B -/-

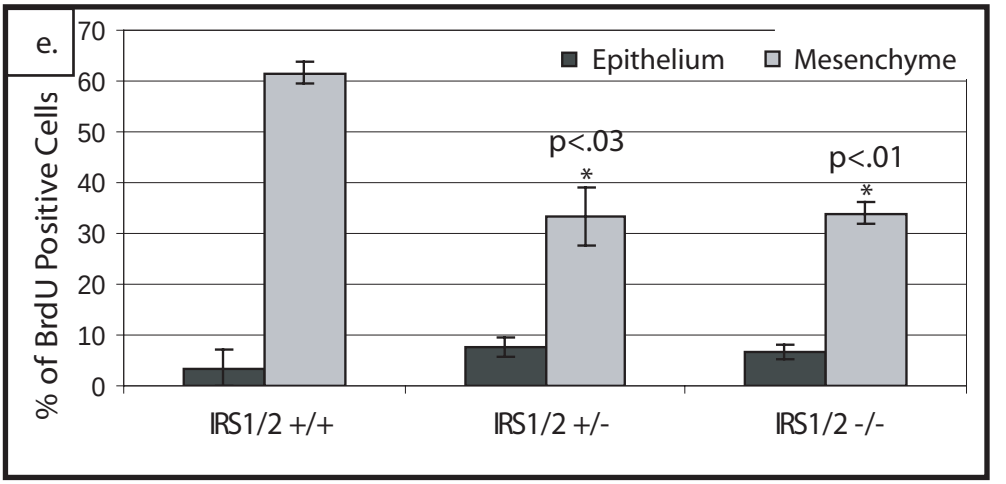
e.
Epithelium
Mesenchyme
% of BrdU Positive Cells
70
60
50
40
30
20
10
0
p<.03
*
p<.01
*
IRS1/2 +/+
IRS1/2 +/-
IRS1/2 -/-